UNIVERSITI
MALAYSIA
KELANTAN

# DISTRIBUTION OF REE IN SOIL LAYER FROM JELI, KELANTAN

**Syahakimi Bin Hasbi**

**J20A0630**

**A reported submitted in fulfilment of the requirements for the degree of Bachelor of Applied Science (Bioindustrial technology) with Honours**

**FACULTY OF BIOENGINEERING AND TECHNOLOGY**

**UMK**

**2024**

# DECLARATION

I declare that this thesis entitled "DISTRIBUTION OF REE IN SOIL LAYER FROM JELI, KELANTAN" is the results of my own research except as cited in the references.

Signature : _____

Student's Name : SYAHAKIMI BIN HASBI

Date : 29 FEBRUARY 2024

Verified by:

Signature : _____

Supervisor's Name : _____

Stamp : _____

Date : _____

# ACKNOWLEDGEMENT

I would like to express my sincere gratitude to the following individuals and organizations for their invaluable support and assistance throughout the completion of this thesis. I am deeply thankful to Prof. Madya ChM. Ts. DR. Abdul Hafidz Bin Yusoff for their guidance, encouragement, financial support provided, and expertise throughout the research process. Their insightful feedback, investment and unwavering support have been instrumental in shaping this work.

I extend my appreciation to the GREAT UMK committee members, Mr Chang Shen Chang, Miss Nazirah, Miss Nadia, and Mr. Taha for their valuable insights and constructive criticism during the thesis defense and throughout my academic journey. He willingness to share their experiences and perspectives has enriched the findings of this thesis.

Lastly, I would be remiss in not mentioning thank my family and friends for their unwavering encouragement, understanding, and patience throughout this endeavor. Their love, support, and belief in me have been a constant source of motivation.

**ABSTRAK**

Elemen Tanah Jarang (REEs) memainkan peranan penting dalam pelbagai aplikasi teknologi, namun distribusi dan kepekatan mereka dalam ekosistem tanah masih kurang difahami. Dalam kajian ini, kami menjalankan analisis komprehensif terhadap pelbagai REEs, termasuk yttrium (Y), lantanum (La), serium (Ce), praseodimium (Pr), neodimium (Nd), samarium (Sm), gadolinium (Gd), terbium (Tb), disprosium (Dy), tulium (Tm), dan ytterbium (Yb), di sepanjang sampel tanah dari pelbagai lokasi. Analisis ini mendedahkan perbezaan spatial dan vertical yang signifikan dalam kepekatan REE dalam profil tanah, menekankan interaksi kompleks antara faktor geologi, geo-kimia, dan alam sekitar yang mempengaruhi taburan REE. Dari segi spatial, pola kepekatan REE yang berbeza diperhatikan di antara lokasi yang berbeza, mengindikasikan sumber tempatan atau formasi geologi yang kaya dengan elemen ini. Selain itu, perbezaan dalam kepekatan REE juga diperhatikan secara vertical dalam profil tanah, mencerminkan proses seperti penumpukan bahan organik, perubahan mineral, dan penyerapan. Penemuan ini menekankan kepentingan analisis tanah yang komprehensif dalam memahami taburan REE dan implikasi ekologi potensinya.

Keywords / Kata Kunci: Rare Earth Elements (REEs), soil layer, geological factors, environmental factors, ecological implications.

## ABSTRACT

Rare earth elements (REEs) play crucial roles in various technological and industrial applications, yet their distribution and implications in terrestrial ecosystems remain poorly understood. This study investigates the spatial and vertical variations in the concentrations of multiple REEs, including yttrium (Y), lanthanum (La), cerium (Ce), praseodymium (Pr), neodymium (Nd), samarium (Sm), gadolinium (Gd), terbium (Tb), dysprosium (Dy), thulium (Tm), and ytterbium (Yb), across soil samples from diverse locations. Through comprehensive soil analysis, it elucidates the complex interplay of geological, geochemical, and environmental factors shaping REE distribution in soils. Spatially, distinct patterns emerge, with certain areas exhibiting elevated REE concentrations indicative of localized sources or geological formations. Vertical variability within soil profiles highlights the influence of processes such as organic matter accumulation, mineral weathering, and leaching on REE distribution across soil layers. These findings underscore the importance of understanding REE dynamics in terrestrial environments for assessing soil fertility, ecosystem health, and potential environmental risks associated with REE accumulation.

Keywords: Rare earth elements, soil samples, spatial variability, vertical distribution,

**TABLE OF CONTENT**

**LIST OF TABLES**

## LIST OF FIGURES

## LIST OF ABBREVIATIONS

| | |
|---|---|
| AC | Air Chanal |
| LE | Legeh |
| G | Gemang |
| DA | Dabong |
| REEs | Rare Earth Elements |
| LREE | Light Rare Earth Elements |
| HREE | Heavy Rare Earth Elements |
| UMK | Universiti Malaysia Kelantan |
| GREAT | Gold, Rare Eartg and Advance Technology |
| ICP-OES | Inductively Couple Plasma-Optical Emission Spectrometry |
| ICP-MS | Inductively Couple Plasma-Mass Spectrometry |

## LIST OF SYMBOLS

| | |
|---|---|
| % | Percentage |
| μm | Micrometer |
| Mm | Millimeter |
| 2 | Square |
| °C | Degree Celsius |
| ° | Degree |
| > | Larger than |
| < | Smaller than |
| = | is equal to |
| g | Gram |
| O | Oxygen |
| La | Lanthanum |
| Ce | Cerium |
| Pr | Praseodymium |

| | |
|---|---|
| Nd | Neodymium |
| Pm | Promethium |
| Sm | Samarium |
| Eu | Europium |
| Gd | Gadolinium |
| Tb | Terbium |
| Dy | Dysprosium |
| Ho | Holmium |
| Er | Erbium |
| Tm | Thulium |
| Yb | Ytterbium |
| Lu | Lutetium |
| Y | Yttrium |
| HF | Hydrofluoric Acid |
| H2O2 | Hydrogen Peroxide |
| $HNO_3$ | Nitric Acid |

| | |
|---|---|
| H3BO3 | Boric Acid |
| Zn | Zinc |
| Hg | Mercury |
| Cd | Cadmium |
| Pb | Lead |
| Cu | Copper |
| Ni | Nickel |
| As | Arsenic |
| Cr | Chromium |
| Al | Aluminum |
| Ba | Barium |
| Co | Cobalt |
| Mn | Manganese |
| Se | Selenium |
| Ag | Silver |

# CHAPTER 1

# INTRODUCTION

## 1.1 Background of Study

Rare Earth Elements (REE) are a group of seventeen chemical elements that include scandium, yttrium, and the fifteen lanthanides. These elements have become increasingly vital in numerous industries, including electronics, renewable energy, and defense. As the demand for REEs continues to rise, understanding their distribution in soil becomes crucial for resource management and sustainable development.

The distribution of REEs in soil plays a significant role in determining the locations with significant REE deposits. By studying the distribution patterns, researchers can identify areas that hold potential for REE extraction. This knowledge can help in optimizing mining activities, reducing environmental impact, and ensuring the efficient utilization of resources.

Moreover, studying the distribution of REEs in soil allows us to comprehend the factors influencing their accumulation. Soil composition, geological processes, and environmental conditions all contribute to the distribution and abundance of REEs. By unraveling these factors, scientists can gain insights into the mechanisms that control the concentration of REEs in the soil.

Understanding the distribution of REEs in soil is not only important for the mining industry but also for environmental management. Some REEs have been associated with environmental pollution and health risks. By studying their distribution in soil, scientists can assess the potential environmental implications and develop strategies to mitigate any negative effects.

Therefore, the study of REE distribution in soil from Jeli Kelantan is of great significance. This region, with its unique geological background and diverse soil composition, presents an intriguing opportunity to explore the distribution patterns and factors affecting REEs. The findings of this study can have far-reaching implications for the future of REE extraction, resource management, and environmental conservation.

## 1.2 Problem Statement

The distribution of Rare Earth Elements (REEs) in soil, while recognized as a critical component of terrestrial geochemical cycles, remains an underexplored and complex subject in environmental science. This study seeks to address several key issues related to REE distribution in soil. The environmental implications of elevated REE concentrations in soil remain poorly understood. While these elements are essential for various industrial and technological applications, their ecological impacts, particularly in terrestrial ecosystems, are not well-documented. This knowledge gap hinders our ability to assess and manage the potential ecological consequences of elevated REEs in soil.

Although REE soil holds immense potential, there are challenges associated with its extraction and utilization. One of the primary challenges is the availability of suitable mineral deposits. REE soil's unique mineral composition requires specific geological conditions, limiting its availability in certain regions.

Additionally, the extraction of REE soil minerals may have environmental implications. Mining operations can disrupt ecosystems, leading to habitat destruction and soil degradation. It is crucial to implement sustainable mining practices and minimize the environmental impact of REE soil extraction.

Furthermore, the utilization of REE soil requires proper education and awareness among farmers and industry professionals. Understanding its benefits and implementing proper soil management practices is essential to maximize the potential of REE soil.

## 1.3 Objectives

With the aim of researching and analyzing soil characteristics and important elements in it, the objectives of this study are:

1.To Investigate and characterize grain size distributions within soil profile layers at selected locations in Jeli, Kelantan.

2. To determine characterize organic matter embedded within the soil profile layers of chosen locations in Jeli, Kelantan.

3. To study the distribution patterns of Rare Earth Elements (REEs) across the soil profiles of Jeli, Kelantan.

## 1.4 Scope of Study

This research focuses on investigating the distribution of Rare Earth Elements (REE) in soil samples collected from selected areas around Jeli, Kelantan. T he research will focus on two distinct geographic regions within Jeli: the vicinity of Air Chanal and the area around Lebuhraya Persekutuan. These locations have been chosen for their geographical diversity and represent a cross-section of the Jeli district, each with its unique environmental conditions, geological formations, and land use practices. By selecting these sites, the study aims to capture a comprehensive view of the distribution of Rare Earth Elements (REEs) in soil in this specific geographic context.

The study will be conducted over a one-month period, commencing in October on the east coast of Malaysia, with an emphasis on seasonal considerations. Sampling will be carried out in various soil layers, categorized as O, A, B, and C, spanning diverse depths to capture a comprehensive representation of soil profiles. Special attention will be given to areas with different land-use histories to capture variations in REE distribution.

Soil characterization will involve a meticulous analysis of grind size, particularly focusing on the O layer, where a higher clay content is anticipated. The investigation will explore the relationship between grind size and the quantities of various soil constituents. A range of grind sizes will be considered to elucidate the impact of particle size on the distribution of REE within the soil matrix.

Furthermore, an loss-of-ignition (loI) method, utilizing particle size analysis with a focus on >32 micron meter, will be employed to determine the percentage of organic matter in the soil samples. Simultaneously, an ICP-MS (Inductively Coupled Plasma Mass Spectrometry) instrument will be utilized to identify and quantify 17 specific elements within the samples, including the targeted REEs. This advanced analytical approach ensures a comprehensive understanding of the elemental composition of the soil.

To interpret the intricate relationships among grind size, organic matter, and REE distribution, statistical and analytical methods will be applied. The ICP-MS results will be subjected to rigorous analysis to identify any correlations or patterns. This holistic approach aims to elucidate the complex interplay between human activities, soil properties, and the distribution of REEs, contributing valuable insights to environmental and geological studies.

This comprehensive scope of study integrates multiple facets, including soil sampling from diverse locations, detailed characterization of soil properties, advanced analytical techniques for elemental identification, and a meticulous analysis of the relationships between grind size, organic matter, and the distribution of REEs. The research is poised to significantly contribute to the understanding of REE dynamics in soil systems, with potential implications for land management, environmental conservation, and sustainable development

## 1.5 Significances of Study

The present study delves into the distribution of Rare Earth Elements (REEs) in the soil of Jeli, Kelantan, with significant implications for environmental analysis, economic growth, and future planning. By exploring the intricate patterns of REE distribution, the research aims to provide valuable insights that extend beyond academic curiosity. From an environmental perspective, understanding these distributions is crucial for assessing potential impacts and fostering sustainable practices to preserve environmental integrity. Simultaneously, economically, the study holds relevance as it contributes to strategic resource utilization, aiding policymakers and industries in making informed decisions regarding resource extraction, thereby fostering economic growth and stability.

Furthermore, the project's emphasis on the future is noteworthy, as it anticipates and addresses potential challenges related to REE availability and sustainability. By providing a foundational resource for future researchers, policymakers, and industries, this research enables the alignment of technological development with environmental conservation and economic prosperity. Utilizing advanced analytical techniques underscores the innovation and rigor of this research, enhancing the accuracy and reliability of findings while contributing to the advancement of analytical methodologies within environmental science. Overall, this FYP project is poised to make substantial contributions to understanding the environmental, economic, and future implications of REE distribution in soil, paving the way for informed decision-making and positive impacts across various sectors.

# CHAPTER 2

# LITERATURE REVIEW

## 2.1 Horizontal Soil Profile

The soil in the Figure 2.1 is a typical soil profile, and it is made up of five main layers, called horizons. These horizons are the result of different soil-forming processes, such as the leaching of organic matter and minerals, the weathering of parent rock, and the activity of soil organisms .

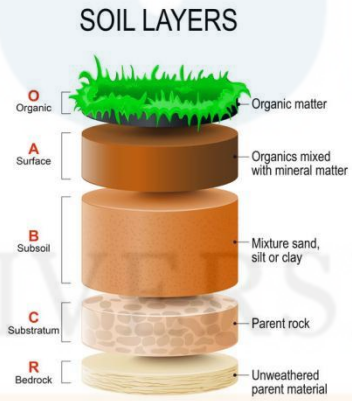


**Figure 0.1: Horizontal Soil Profile**

(Source: Soil is the thin layer of material covering the earth's surface, 2020)

The O horizon, also known as the litter layer, is the uppermost layer of the soil profile and plays a crucial role in the overall health and functionality of the soil ecosystem. Comprised mainly of fresh and decomposing organic matter, such as fallen leaves, twigs, and dead plants, the O horizon is a dynamic and constantly changing layer. The layer of organic material helps shield the soil from erosion caused by wind and water. By providing a physical barrier, the O horizon prevents the loss of valuable topsoil, which is rich in nutrients and essential for plant growth. The O horizon serves as a reservoir of nutrients. As organic

matter decomposes, it releases essential elements and compounds into the soil. These nutrients, such as nitrogen, phosphorus, and potassium, are vital for the growth and development of plants. The statement mentions that sediments have been transported by wind and water (Mihajlovic et al., 2019), leading to the development of a soil profile that is deficient in finer particles like clay and silt. This has implications for the distribution of REEs because fine particles in the soil are often more reactive and prone to chemical weathering. The absence of these fine particles in the soil may contribute to the observed low concentrations of REEs in the O horizon.

The A horizon, or topsoil, is a crucial layer for plant growth, as it is rich in organic matter, humus, and nutrients. In the context of Rare Earth Elements (REEs), the concentration and distribution of these elements in the topsoil can be influenced by several factors.The statement mentions that the topsoil generally contains moderate REE concentrations. The source of REEs in the topsoil can be attributed to the underlying parent material, which serves as the initial source of these elements. The mineral composition of the parent material contributes to the baseline concentration of REEs in the topsoil. Different types of rocks and minerals may have varying levels of REEs. The statement notes that the topsoil may be potentially enriched by eluviation (Michael E. Ritter, 2021), which is the downward movement of materials from upper horizons. In the context of REEs, this means that certain elements may be leached from upper horizons (like the O horizon) and accumulate in the topsoil. The leaching process can selectively transport certain elements while leaving others behind. The specific REEs present in the topsoil would depend on the geological characteristics of the parent material and the regional environment. The concentration of each element can vary based on factors such as the original rock composition, weathering processes, and the presence of organic matter.

The B horizon, or illuviation horizon, is located below the A horizon (topsoil) and is known for accumulating materials leached down from upper horizons. The statement correctly notes that the B horizon can exhibit enrichment in Rare Earth Elements (REEs), particularly heavy REEs. This enrichment is attributed to the tendency of REEs to form insoluble complexes with clay minerals. Clay minerals in the soil have a high surface area and a net negative charge. Rare Earth Elements, being trivalent cations, can form stable complexes with these clay minerals. The heavy REEs, which include elements like europium, gadolinium, terbium, dysprosium, and erbium, are often less mobile than their lighter counterparts due to their larger atomic size and greater affinity for adsorption onto clay minerals (Albrecht, 2015). As water moves through the soil profile, leaching materials from upper horizons (such as the A horizon), the REEs can be transported downward. In the B horizon, where clay minerals accumulate, the REEs are more likely

to form complexes with these minerals and become less mobile. This can lead to an enrichment of REEs in the B horizon compared to the overlying horizons.

The C horizon, often referred to as the parent material horizon, is the lowest layer of the soil profile and is composed of the weathered remains of the underlying rock. As mentioned, the C horizon is generally not very fertile, and it is not the primary zone where most plant roots grow. The statement correctly notes that the parent material in the C horizon usually holds the highest concentrations of Rare Earth Elements (REEs) in the soil profile. This is because weathering processes haven't significantly mobilized the REEs yet. In the C horizon, the original minerals from the underlying rock may still contain relatively high concentrations of REEs. Weathering involves the physical and chemical breakdown of rocks over time (Yusoff et al., 2013). During this process, minerals in the rock release various elements, including REEs. However, in the C horizon, where the weathering is not as advanced, the REEs are still associated with the parent material, and their concentrations may be higher compared to the overlying horizons. As water percolates through the soil profile and undergoes weathering, it can transport elements from the C horizon to the upper horizons, influencing the distribution and concentration of REEs in the soil profile. The fact that the C horizon is not very fertile and not the main area for plant roots indicates that, while the C horizon may contain high concentrations of REEs, these elements may not be readily available for plant uptake. Analyzing the REE content in the C horizon is essential for understanding the geological context of a particular area and can contribute to studies of soil formation, mineral weathering, and potential environmental impacts. Techniques such as geochemical analysis and mineralogical studies can help characterize the REE content in the C horizon and provide insights into the broader soil profile dynamics.

## 2.2 Mechanisme Formation of Soil

The formation of soils enriched with Rare Earth Elements (REEs) is a multifaceted process shaped by geological, chemical, and biological mechanisms (Fisher, 2017). It commences with the weathering of parent rocks, which contain minerals housing REEs. Mechanical weathering, including freeze-thaw cycles and pressure changes, breaks down rocks into smaller particles, while chemical weathering processes release REEs into the soil solution. Rainfall-induced leaching carries these elements downward through the soil profile. The illuviation (B) horizon, enriched by leached materials, becomes a focal point for REE accumulation due to their tendency to form insoluble complexes with clay minerals. Climate conditions, such as temperature and rainfall, influence the rate of weathering and leaching, affecting REE mobility. Organic matter and vegetation, including nutrient-cycling plants and soil microorganisms, contribute

significantly. Plants extract REEs from the soil, and upon decomposition, add organic matter to create a nutrient-rich environment. Root exudates and microbial activity further influence REE mobility. As water moves through the soil, REEs may adsorb onto clay minerals or form complexes with organic matter, affecting their distribution (Zhenghua et al., 2001). Over time, these processes lead to the development of distinct soil horizons, each with varying concentrations of REEs. The intricate interplay of geological, climatic, and biological factors contributes to the diversity observed in soils containing REEs worldwide. Understanding these mechanisms is vital for unraveling the complexities of soil formation and ecosystem dynamics.

## 2.3 Geological Background of Jeli, Kelantan

Jeli, Kelantan is a district located in the northeastern part of Peninsular Malaysia. It is situated in the state of Kelantan, known for its rich natural resources and diverse landscapes. The geological background of Jeli plays a crucial role in shaping the distribution of REEs in the soil (Anak Rebu et al., 2023). The region is primarily composed of granitic rocks, which are known to contain significant concentrations of REEs. These granitic rocks were formed through the process of magmatic differentiation, where the molten rock cools and solidifies, leading to the crystallization of minerals (Earle & Earle, 2015) rich in REEs. In addition to granitic rocks, Jeli also contains sedimentary rocks such as sandstone and shale. These rocks have different mineral compositions and geological origins, which can influence the distribution of REEs in the soil. The interaction between these different rock types, along with weathering processes, determines the availability and mobility of REEs in the soil. The diverse geological background of Jeli, Kelantan provides a unique opportunity to study the distribution of REEs in different soil types. By analyzing samples from various locations within the region, researchers can gain insights into the factors influencing the accumulation of REEs and the potential for resource extraction.

## 2.4 Organic Matter

Organic matter in soil is a vital component that comprises the remains of once-living organisms and their byproducts in various stages of decomposition. It is a dynamic and essential part of the soil ecosystem, influencing soil structure, fertility, and overall health. Organic matter includes a diverse array of materials, such as decomposed plant and animal residues, microbial biomass, and other organic

substances. These organic compounds are rich in carbon and nutrients, serving as a source of energy for soil microorganisms. As organic materials break down, they release essential nutrients like nitrogen, phosphorus, and sulfur into the soil, contributing to the nutrient cycling crucial for plant growth ( Alexandra Bot, 2024). Additionally, organic matter plays a key role in soil structure by promoting the formation of aggregates, enhancing water retention, and improving drainage. The carbon in organic matter is also a significant component in the global carbon cycle, with practices that enhance organic matter content contributing to carbon sequestration and climate change mitigation.

The decomposition of organic materials in soil by living organisms is a dynamic and essential process that influences soil structure, nutrient availability, and overall soil fertility. As organic residues are broken down, they release a multitude of nutrients crucial for plant growth. Simultaneously, the organic chemical compounds produced during this decomposition contribute to soil structure by binding soil particles together. Fresh residues contain a diverse array of organic molecules, including proteins, amino acids, sugars, and starches (Van Es, 2021). These compounds are considered part of the fresh organic matter. However, their presence in the soil is relatively short-lived because of their structural characteristics, which make them highly susceptible to decomposition. Microorganisms thriving in the soil utilize these organic molecules as a source of energy and nutrients, breaking them down rapidly. Some cellular molecules, such as lignin, have a more complex structure that makes them resistant to decomposition. Lignin takes longer for microorganisms to break down, resulting in its accumulation in the soil over time. This is particularly evident in poorly drained soils like peats and mucks, as well as in wetlands that have been converted into agricultural areas. In these waterlogged conditions, the decomposition process is impeded, leading to the accumulation of significant amounts of organic matter. While poorly drained soils and wetlands can hold large quantities of organic matter due to limited decomposition caused by waterlogging, it's important to note that the organic molecules in such environments may not provide the same immediate benefits as fresh residues. The structural complexity of certain molecules, like lignin, makes them resistant to decomposition, and as a result, they may not contribute as readily to nutrient release and other soil health benefits.

## 2.5 Soil Partical Size

The size of soil particles, ranging from larger grains like sand and silt to smaller particles like clay, significantly influences the distribution and mobility of REEs within the soil profile. Physically, larger grains, such as sand and silt, generally exhibit lower REE concentrations due to their reduced surface area

compared to finer particles (Sandra Brown, 2021). These larger grains predominantly host REEs associated with primary minerals like quartz and feldspar, which are less prone to weathering. In contrast, smaller grains like clay possess a significantly larger surface area, providing more sites for REE adsorption. Clay minerals, such as smectites and illites, with negatively charged surfaces, attract and bind REE ions, particularly the heavier lanthanides.

Chemically, the accessibility of REEs is influenced by grain size. Finer-grained fractions undergo more effective weathering processes (Rocchi et al., 2017), such as hydrolysis and oxidation (Yu et al., 2023), liberating REEs from minerals and enhancing their mobility. Coarser grains, however, experience slower REE release due to less pronounced weathering effects.

Sorption and mobilization dynamics further shape the relationship between grain size and REEs. Clay minerals play a pivotal role in retaining REEs, with strong adsorption onto their surfaces hindering the movement of REEs and leading to enrichment in the B horizon where fine particles accumulate. Organic matter, though generally exhibiting weaker adsorption compared to clay, also influences REE behavior by complexing with certain REE ions and contributing to their retention in the A horizon.

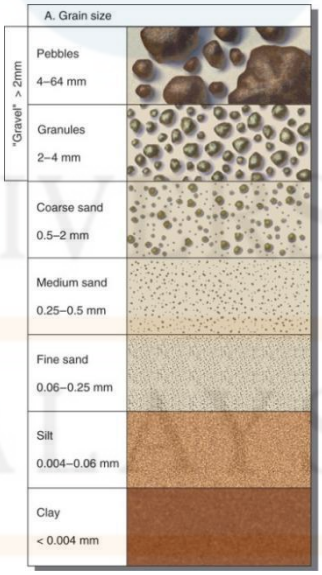


**Figure 0.2: Soil Classification Chart.**

**(Source: Grain size distribution., 2015)**

Starting with pebbles larger than 4mm, these are relatively large and contribute to the soil's physical structure, affecting aspects such as drainage and aeration. Granules, falling within the 2-4mm range, are smaller than pebbles but still contribute to the soil's structure and can influence water movement. Moving into the sand fractions, we encounter Very Coarse Sand (1mm-2mm), Coarse Sand (710µm-1mm), Medium Coarse Sand (500µm-710µm), and Medium Sand (355µm-500µm). These sand fractions are crucial in determining the soil's texture, influencing properties like permeability and water retention. Coarser sands enhance drainage, while finer sands contribute to water retention. The progression continues with Fine Sand (125µm-250µm) and Very Fine Sand (63µm-125µm), where the particles become finer. These fractions further influence soil texture, impacting its ability to hold nutrients and support plant growth. The shift from coarse to fine sands reflects changes in the soil's ability to retain water and nutrients. Beyond the sand fractions, we encounter the transition into silt and clay. Coarse Silt comprises particles ranging from 32µm to 63µm, contributing to the soil's fine texture. Medium and Fine Silt, along with Clay particles smaller than 32µm, represent the finer fractions. These fine particles have high surface areas and play a crucial role in nutrient retention, water-holding capacity, and overall soil fertility.

## 2.6 Digestion

Sample digestion is a critical step in the laboratory analysis of soil samples for (REEs) and other elements. During this process, the soil samples are prepared and chemically treated to break down the soil matrix and release the elements of interest. In the case of REEs, sample digestion typically involves the use of strong acids, such as hydrochloric acid (HCl), nitric acid (HNO3), and hydrofluoric acid (HF), to dissolve the solid soil material. These acids effectively break the chemical bonds in the sample, liberating the REEs and allowing them to be quantified accurately through subsequent analytical techniques. The digestion process is usually carried out in specialized containers, such as Teflon digestion vessels or acid-resistant glass beakers, in controlled conditions. The temperature and time of digestion can vary depending on the specific analytical method and the nature of the samples. Often, microwave-assisted digestion systems are employed to speed up the process and ensure uniform digestion.

In soil digestion for the analysis of heavy metals and other soil components, researchers commonly use various acids to break down organic and inorganic materials. The choice of acids depends on the specific characteristics of the soil and the elements of interest. (Chen et al., 2014) utilized a digestion method

involving a combination of HNO3 and HF to dissolving a wide range of sample matrices and is particularly suitable for determining the total concentration of heavy metals, (Jian et al., 2007) selected HNO3, HCl, and H2O2 to digest marine sediment samples. This combination is often employed to ensure the complete dissolution of organic and inorganic components in sediments. The satisfactory results indicate the suitability of this digestion system for marine sediment analysis. (Liang et al., 2012) applied a digestion system comprising HNO3, H2O2, and HF to detect the concentrations of nine heavy metals in stream sediment. Hydrofluoric acid is particularly useful in breaking down silicate minerals and facilitating the release of heavy metals from sediment matrices. This method is valuable for analyzing heavy metals in complex geological samples (Qiu et al., 2016). The choice of this method reflects its adequacy for handling diverse heavy metal species.

The combination of these acids in digestion methods is known as acid digestion, and it is aimed at breaking down soil samples into a solution that can be analyzed for various elements, including heavy metals. The choice of acids and their concentrations depend on the specific goals of the analysis, the types of elements being targeted, and the nature of the soil matrix. The choice of this method reflects its adequacy for handling diverse heavy metal species. HNO3 is a strong oxidizing acid that serves multiple functions. It helps in decomposing organic matter, oxidizing most metals, and facilitating the solubilization of a wide range of elements. It is a versatile acid in soil digestion due to its effectiveness in breaking down various sample components, it can digest a broad spectrum of elements, including but not limited to metals such as aluminum, iron, copper, and zinc. HF is effective in breaking down silicate minerals, which are common in soil. It is particularly useful for dissolving minerals containing elements like aluminum and silicon. HF can digest silicon and aluminum, among other elements found in silicate minerals (Rogers & Bennett, 2004). HCl aids in the dissolution of minerals, particularly those that may contain metals of interest. It assists in the liberation of certain metals and is often used in conjunction with nitric acid as aqua regia, a powerful digestion mixture. Hydrochloric acid can digest metals like calcium, magnesium, and some transition metals. H2O2 is often added to digestion mixtures to enhance the oxidation of organic matter. It can improve the efficiency of digestion by breaking down organic compounds. Hydrogen peroxide assists in the digestion of organic matter but is not a primary acid for dissolving metals.

## 2.7 REE

Rare Earth Elements (REEs) are a group of 17 chemical elements encompassing both the light rare earth elements (LREEs) and heavy rare earth elements (HREEs). LREEs include Cerium (Ce), Lanthanum (La), Praseodymium (Pr), Neodymium (Nd), Promethium (Pm), and Samarium (Sm), while HREEs consist

of Europium (Eu), Gadolinium (Gd), Terbium (Tb), Dysprosium (Dy), Holmium (Ho), Erbium (Er), Thulium (Tm), Ytterbium (Yb), and Lutetium (Lu). Additionally, Yttrium (Y) is often considered alongside REEs due to its comparable chemical properties. These elements share similarities in their chemical behavior, being trivalent with three valence electrons, which contributes to their cohesive categorization. Despite their name, REEs are not inherently rare in occurrence; however, they are often dispersed in low concentrations throughout the Earth's crust, necessitating sophisticated extraction methods for practical use. Their significance lies in their diverse applications across industries, ranging from electronics and catalysis to lighting and medical imaging.

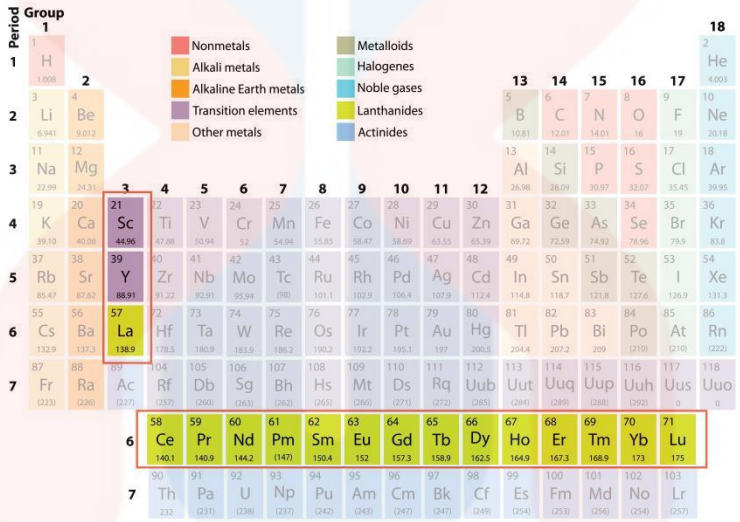


**Figure 2.3: Rare Eearth Element in Periodic Table**

**(Scource: Rare earth elements, n.d.)**

Chemically, REEs exhibit unique properties that make them valuable in various technological applications. The trivalent nature of REEs, characterized by their outermost shell having three electrons, allows them to form stable compounds and exhibit magnetic and luminescent properties (Linert et al., 2003). The combination of these properties makes certain REEs crucial for the development of advanced technologies, such as super-strong magnets for electric vehicles and wind turbines. Additionally, REEs play a pivotal role in the fields of metallurgy, catalysis, and materials science due to their unique electronic configurations. While REEs are not uniformly distributed globally, with China historically dominating production (Wall, 2021), ongoing research focuses on diversifying supply sources and improving extraction processes to ensure a sustainable and stable supply chain for these critical elements. Advances in recycling and responsible mining practices are also gaining attention to address both environmental concerns and potential geopolitical implications associated with REE production.

The upper continental crust, which includes the Earth's landmasses, is enriched with REEs due to various geological activities, such as weathering, erosion, and the deposition of sediments over geological time scales. These processes contribute to the accumulation of REEs in minerals and rocks that form the upper crust. On the other hand, the lower crust and mantle, being subjected to high temperatures and pressures, undergo differentiation processes that lead to a comparatively lower concentration of REEs (Hoshino et al., 2016). The crustal composition is not homogenous, and different regions exhibit variations in REE abundance. The upper continental crust, particularly in areas with granitic rocks, tends to have higher concentrations of REEs. This geochemical distribution has implications for exploration and extraction efforts, as regions with elevated REE concentrations in the upper continental crust may be more economically viable for mining activities.

## 2.8 Instrument

### 2.8.1 Microwave Digetion

Microwave digestion is a sample preparation technique widely used in analytical chemistry to dissolve solid samples, such as soil, for subsequent analysis of elements by methods like inductively coupled plasma mass spectrometry (ICP-MS) or inductively coupled plasma optical emission spectrometry (ICP-OES). This method allows for the rapid and efficient decomposition of complex matrices, facilitating accurate determination of element concentrations in the sample. Microwave digestion involves exposing the sample to microwave radiation, which rapidly heats the sample and accelerates the digestion process (Matusiewicz, 2019). The key components of this process include the sample, a digestion vessel, and a mixture of acids.

a) **Microwave Source**

The system includes a microwave generator that produces microwave radiation. Microwaves are electromagnetic waves with frequencies between 300 MHz and 300 GHz. In microwave digestion systems, the frequency used is typically in the range of 2.45 GHz.

b) **Digestion Vessels**

The sample to be digested is placed in specialized digestion vessels that are suitable for exposure to microwave radiation. These vessels are designed to withstand the high temperatures and pressures generated during the digestion process.

c) **Acid Mixture**

An acid mixture, often composed of nitric acid ($HNO_3$) and hydrochloric acid (HCl), is added to the sample. The acids play a crucial role in breaking down organic and inorganic components of the sample, facilitating the release of elements into solution.

d) **Microwave Irradiation**

The digestion vessels containing the sample and acid mixture are arranged in the microwave digestion system. When microwaves are emitted, they penetrate the digestion vessels and interact with the sample. The microwaves induce molecular motion and generate heat through dipole rotation and ionic conduction.

e) **Temperature and Pressure Control**

The microwave system carefully controls the temperature and pressure within the digestion vessels. The rapid and uniform heating of the sample ensures efficient digestion. The elevated pressure aids in preventing the loss of volatile components.

f) **Chemical Reactions**

The combination of heat and the acidic environment initiates chemical reactions that break down complex organic and inorganic compounds in the sample. These reactions result in the dissolution of minerals and the liberation of elements into the solution.

g) **Cooling and Filtration**

After the digestion process is complete, the vessels are allowed to cool. The cooling phase is crucial to stabilize the system and prepare the sample for subsequent processing. The resulting solution, now containing the dissolved elements, is typically filtered to remove any remaining solid particles. The clear filtrate is then ready for analysis.

### 2.8.2 Coupled Plasma Mass Spectrometry (ICP-MS)

ICP-MS is an analytical technique that combines inductively coupled plasma and mass spectrometry to determine the elemental composition of a sample. The detection and quantification of trace elements and isotopes in a wide range of samples . This instrumental method combines inductively coupled plasma (ICP) with mass spectrometry (MS) to achieve high sensitivity, precision, and the capability to analyze multiple elements simultaneously (Wilschefski & Baxter, 2019). ICP-MS operates by ionizing elements in a sample using an inductively coupled plasma source and then separating and quantifying the ions based on their mass-to-charge ratio. The process allows for simultaneous measurement of multiple elements.

**a) Inductively Coupled Plasma (ICP):**

ICP is a high-temperature plasma source generated by the inductive coupling of radiofrequency energy. Typically, argon gas is used to create a plasma with temperatures exceeding 10,000 Kelvin. In this state, the sample introduced into the plasma is ionized, forming cations.

**b) Ionization and Atomization:**

The high temperatures of the ICP cause the atoms in the sample to become ionized. This ionization process results in the formation of positively charged ions (cations). Concurrently, the sample undergoes atomization, breaking down the molecular structure into individual atoms.

**c) Mass Spectrometry (MS):**

The ionized and atomized species from the ICP are then introduced into the mass spectrometer. In the mass spectrometer, ions are separated based on their mass-to-charge ratio

(m/z). ICP-MS typically employs a quadrupole mass filter, a magnetic sector, or a time-of-flight (TOF) analyzer for this purpose.

**d) Detector**

The separated ions are directed to a detector, where their abundance is measured. The intensity of the signals corresponds to the concentration of the specific isotopes or elements present in the sample.

**e) Isotopic Analysis**

ICP-MS is particularly valuable for isotopic analysis, as it can distinguish between different isotopes of an element based on their mass differences. Isotopic analysis is a powerful technique that involves studying the variations in the masses of isotopes of a particular element. Isotopes are atoms of the same element that have the same number of protons but different numbers of neutrons.

### 2.8.3 Inductively Coupled Plasma Optical Emission Spectroscopy (ICP-OES)

Inductively Coupled Plasma Optical Emission Spectroscopy (ICP-OES) is an analytical technique used for the simultaneous qualitative and quantitative determination of elements present in a sample. Here's a breakdown of how the instrument works:

**a) Inductively Coupled Plasma (ICP)**

The sample is first introduced into an extremely hot (~10,000 K) and ionized gas known as the inductively coupled plasma (ICP). The ICP is generated by passing an inert gas, typically argon, through a radiofrequency (RF) coil, creating a high-energy plasma. In the plasma, the sample undergoes complete atomization, resulting in the formation of free atoms and ions.

### b) Optical Emission Spectroscopy (OES)

As the atoms and ions in the plasma return to their ground state, they emit characteristic electromagnetic radiation. The emitted radiation is collected and passed through a spectrometer, where it is dispersed into its component wavelengths using a diffraction grating or prism. The dispersed radiation is then detected by a detector array, such as a charge-coupled device (CCD) or photomultiplier tube (PMT).

### c) Qualitative and Quantitative Analysis

The wavelengths of the emitted radiation correspond to the characteristic spectral lines of the elements present in the sample. By measuring the intensity of these spectral lines, the concentration of each element can be determined. Calibration curves are typically constructed using standards of known concentration for each element of interest, allowing for accurate quantification. The simultaneous measurement of multiple elements in the sample enables comprehensive elemental analysis.

### d) Instrument Components

The main components of an ICP-OES instrument include the sample introduction system, plasma source, optical system, and detector. The sample introduction system may consist of a nebulizer, spray chamber, and peristaltic pump to deliver the sample into the plasma. The optical system comprises lenses, mirrors, and a grating or prism to disperse the emitted radiation. The detector array converts the dispersed radiation into electrical signals, which are then processed and analyzed by software.

### e) Advantages of ICP-OES:

High sensitivity: ICP-OES can detect elements at trace levels, typically in the parts per billion (ppb) or parts per million (ppm) range. Wide elemental coverage: It can simultaneously analyze multiple elements across the entire periodic table. Speed and precision: ICP-OES provides rapid analysis with high precision

and accuracy, making it suitable for routine and research applications in various industries such as environmental monitoring, pharmaceuticals, and metallurgy.

# CHAPTER 3

## MATERIALS AND METHODS

The material utilized for sample collection and analysis involves a set of carefully chosen tools and equipment to ensure precision and efficiency. For sample collection, the sampling equipment includes zip lock plastic bags, a hand shovel, gloves for personal protection, and an auger for soil retrieval. The apparatus for subsequent analysis encompasses disposable aluminum foil for secure packaging, a rubber hammer for sample preparation, an oven for controlled drying, an ultrasonic water bath for sample dispersion, an ASTM sieve set and air jet for particle size analysis, a mechanical shaker for agitation, and polyethylene sample bags for storage. The materials involved in the digestion process comprise a hotplate for controlled heating, Teflon containers to resist chemical reactions, a fume chamber to ensure safety, beakers with lids, micropipettes and tips for precise measurements, Falcon tubes, polypropylene containers, and chemicals can refer at Table 3.1 such as boric acid, hydrofluoric acid, hydrogen peroxide, and nitric acid. Personal protection, particularly when handling acids, is paramount and necessitates the use of appropriate safety gear. The software employed for data organization and visualization is Microsoft Excel, while ArcMap serves as a robust tool for geochemical data visualization. The careful selection of these materials and tools contributes to the reliability and accuracy of the analytical processes involved in the study.

**Table 3.1: List of Chemical and Reagent**

| No | Chemical and Reagents | Symbols |
|---|---|---|
| 1 | Boric Acid | H3BO3 |
| 2 | Hydrofluoric Acid | HF |
| 3 | Hydrogen Peroxide | H2O2 |
| 4 | Nitric Acid ($HNO_3$) | $HNO_3$ |
| 5 | Hydrochloric acid | HCL |
| 5 | De-ionised water | - |

## 3.1 Selection and Sampling Sites

The meticulous selection of sites within the Jeli district, including the proximities of Tebing Sg Chanal, Air Chanal, Legeh, and Dabong, holds profound significance in unraveling the intricacies of soil composition. Soil was taken by 14 and 16 October 2023. Particularly noteworthy is the distinct soil profile in the Dabong area, characterized by well-defined layers ranging from O to B horizons, offering a natural laboratory for comprehensive analysis. Of particular interest is the convergence of residential areas around Gemang, presenting a unique opportunity to explore the interface between human activity and soil composition. At each sampling point, collect soil samples from multiple depths to obtain a vertical profile of the soil's REE distribution. Ensure proper labeling of collected samples, including information about the sampling depth and location. Refer Figure 3.1 for location sampling that have been taken and Table 3.2 for coordinates point sampling. Remove any visible contaminants, such as roots or rocks, from the collected soil samples. Air-dry the samples at room temperature to prevent contamination by moisture. Once dried, store the samples in airtight using zip lock plastic bags, labeled containers to prevent contamination and moisture absorption. Properly package the samples to ensure their integrity during transport to the laboratory

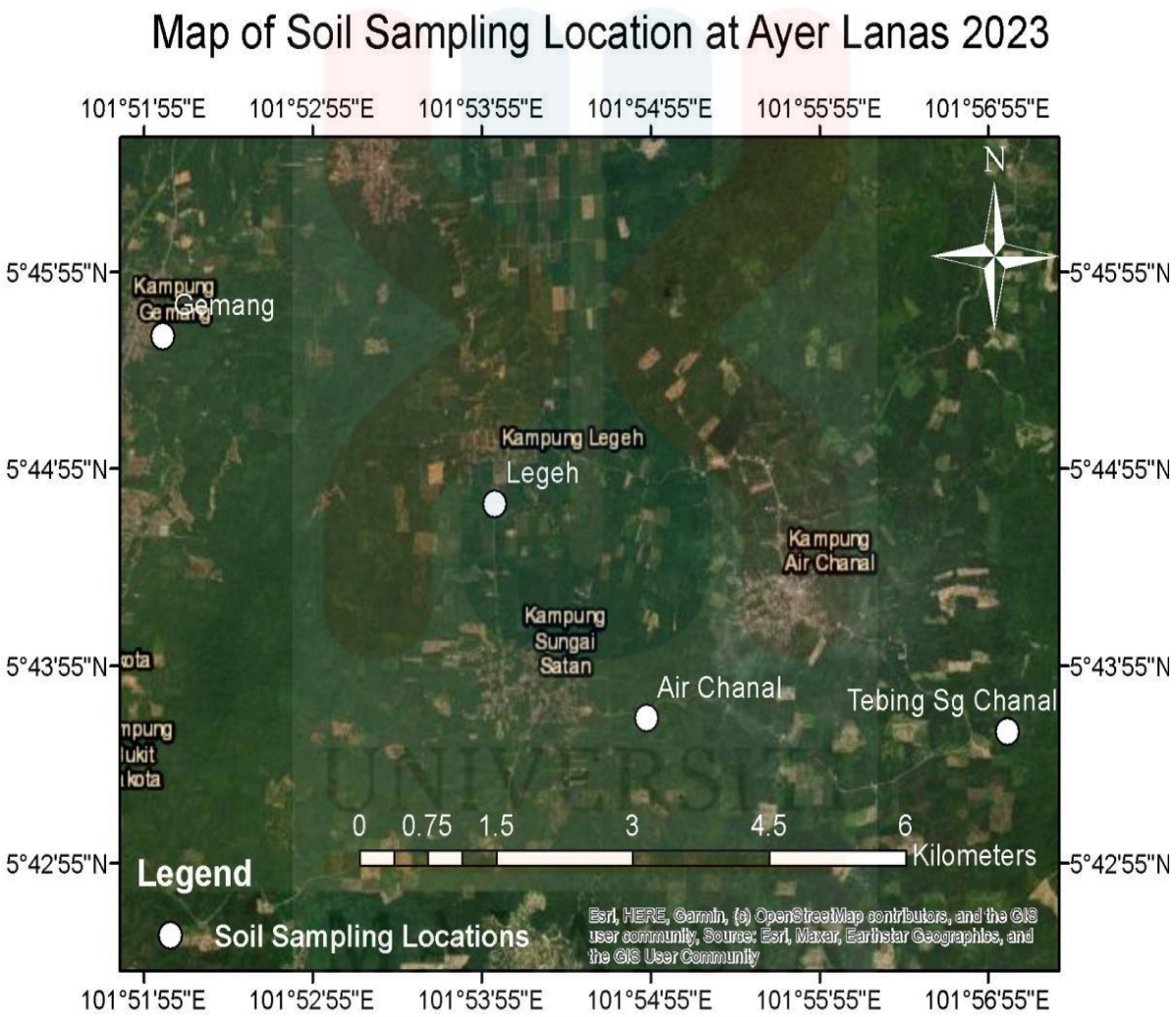


**Figure 3.1: Location sample take**

**Table 3.2: Coordinate Sampling**

| Place | Sample Lable | Latitude | Longitude |
|---|---|---|---|
| Tebing Sg Chanal | AC01S-O<br>AC01S-A | 5°43'34.44"N | 101°57'3.96"E |
| | AC01S-B-C | 5°43'35.274"N | 101°571.794"E |
| Air Chanal | AC02S0-0<br>AC02S0-AB<br>AC02S-B | 5°43'39.174"N | 101°54'53.226"E |
| Legeh | LE03S-A<br>LE03S-B | 5°44'44.388"N | 101°53'59.604"E |
| Gemang | G04S-A | 5°45'35.532"N | 101°52'0.912"E |
| | G04S-B | 5°45'35.52"N | |
| Dabong | DA04S-O<br>DA04S-A1<br>DA04S-B1 | 5°14'41.136"N | 102°15'18.18"E |
| | DA04S-A2<br>DA04S-B2 | 5°14'42.918"N | 102°15'18.396"E |

## 3.2 Lab Analysis

Conduct the laboratory analysis of the soil samples to measure REE concentrations.

### 3.2.1 Moisture Analysis

To assess the moisture content in the soil samples, a meticulous step-by-step procedure was followed. Initially, the freshly collected soil samples were spread out in a thin layer to allow for uniform drying. Before enter to the oven soil sample was weighed by using analytical balance. These samples were then placed in an oven set at a standardized temperature of 105°C. This temperature was chosen to ensure efficient removal of moisture while minimizing the risk of altering the soil's chemical composition. The samples were left to dry in the oven until a constant weight was achieved, indicating that all moisture had been removed. This critical step helped eliminate variability in moisture content between samples, ensuring the accuracy of subsequent analyses. Once the samples attained a constant weight, signifying complete drying, they were carefully removed from the oven and allowed to cool to room temperature in a desiccator to prevent moisture absorption from the surrounding environment.

### 3.2.2 Grind Size Analysis

The grain size analysis of soil samples involved a systematic and precise procedure. Initially, the dried soil samples were carefully crushed into small pieces using a hammer, ensuring uniformity in particle size. This crushing process facilitated the subsequent separation of soil particles based on their size distribution. The soil samples were sieved using a series of stainless steel sieves with progressively finer mesh sizes, including 4mm, 2mm, 1mm, 710µm, 500µm, 355µm, 250µm, 125µm, 63µm, and 32µm. Each sieve was stacked in descending order of mesh size, allowing for the sequential separation of soil particles. The sieving process was conducted using a mechanical shaker to ensure consistent and thorough separation of particles. After sieving, the retained material on each sieve was carefully weighed to determine the percentage of soil particles within each size fraction. Notably, the finest fraction passing through the 32µm mesh size was collected for further analysis, as it contains crucial information about the distribution of fine-grained particles in the soil.

### 3.2.3 Organic Matter Analysis

Following the grain size analysis, the <32 micron fraction was utilized for the identification of organic matter content through the Loss on Ignition (LOI) method. The LOI method involves a series of meticulous steps to accurately determine the organic matter content in soil samples. Initially, the <32 micron soil fraction obtained from the grain size analysis was carefully weighed into pre-weighed crucibles. These crucibles containing the soil samples were then placed into a muffle furnace and heated at a controlled temperature typically ranging between 400°C to 550°C. During heating, organic matter within the soil samples undergoes combustion, resulting in the release of carbon dioxide and other volatile compounds. The heating process continues until all organic matter is completely oxidized, leaving behind only inorganic residues. Subsequently, the crucibles containing the soil samples were removed from the furnace and allowed to cool in a desiccator to prevent moisture absorption from the surroundings. Once cooled, the crucibles were reweighed to determine the loss in weight due to the combustion of organic matter. The percentage of organic matter lost during ignition, commonly referred to as the LOI, was then calculated using the formula:

$$\text{LOI } (\%) = \left(\frac{Initial\ Weight - Final\ Weight}{Initial\ Weight}\right) \times 100$$

Where "Initial weight" represents the weight of the crucible and soil sample before ignition, and "Final weight" represents the weight of the crucible and residual inorganic material after ignition. By accurately measuring the weight loss after ignition, the LOI method provides a reliable estimate of the organic matter content in soil samples. This meticulous procedure ensures the precise determination of organic matter content, essential for understanding soil fertility, nutrient cycling, and carbon storage dynamics.

### 3.2.4 REE Analysis

**Sample Digestion**

Weigh and To digest soil samples for the analysis of organic matter content using the <32 micron fraction, a method involving HF, H2O2, and HNO3 was employed. The digestion process involves a series of meticulous steps to ensure the complete dissolution of organic and inorganic components in the soil samples. Initially, 0.5g of each soil sample from the <32 micron fraction was accurately weighed into digestion vessels. Subsequently, a mixture of HF, H2O2, and HNO3 was prepared in a fume hood, following prescribed safety protocols due to the corrosive and hazardous nature of these chemicals. The digestion process continued by adding a predetermined volume of the HF-H2O2-HNO3 mixture to the soil samples in the digestion vessels. The addition of HF serves to dissolve silicate minerals, facilitating the release of bound organic matter and trace elements. H2O2 acts as an oxidizing agent, aiding in the decomposition of organic matter and the oxidation of certain metals. HNO3 acts as a strong oxidizing acid, assisting in the dissolution of metals and converting organic nitrogen into nitrate.

The digestion vessels containing the soil samples and the digestion mixture were then tightly sealed and subjected to controlled heating. The heating process was carried out gradually to avoid violent reactions and ensure thorough digestion of the soil samples. Typically, a combination of hotplate heating and microwave digestion techniques may be employed to accelerate the digestion process. During digestion, the soil samples underwent chemical decomposition, resulting in the release of gases and the formation of soluble metal and mineral complexes in the digestion solution. The heating process continued until the digestion solution became clear or colorless, indicating the completion of sample digestion.

Following the addition of boric acid and other acids, the solution was heated once again to ensure thorough mixing and dissolution of the added reagents.Following digestion, the digested solutions were allowed to cool to room temperature before transferring them to falcon tube for the ICP-MS analysis. Careful handling and disposal procedures were followed to ensure safety and environmental compliance due to the hazardous nature of the digestion reagents.

# CHAPTER 4

# RESULTS AND DISCUSSION

## 4.1 Moisture

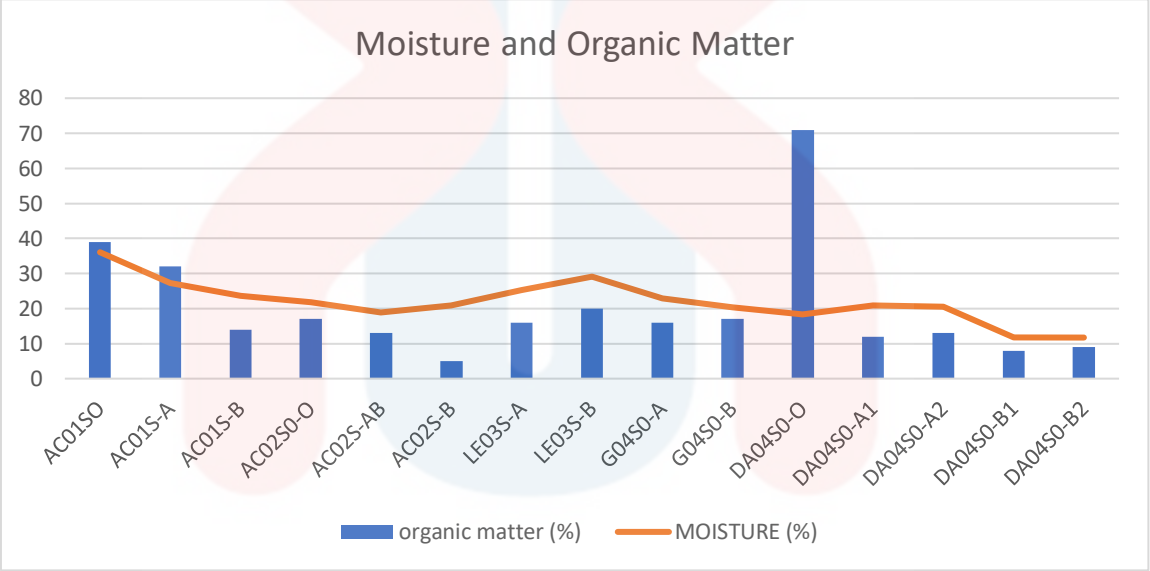


**Figure 4.1 : Moisture and Organic Matter Content in Soil Sample**

In the first location, the highest moisture content was recorded in sample AC01S-O at 36.06%, with an initial sample weight of 211.84g reduced to 135.45g after heating, indicating a loss of 76.39g. Conversely, the lowest moisture percentage was found in sample AC01S-B, at 23.66%. It is noteworthy that the organic matter content in sample AC01S-O was higher than in AC01S-B. Higher organic matter content can lead to increased air absorption, while lower mineral content may result in reduced air absorption. The soil sample from location AC01S recorded the highest initial sample weight of 702.21g, decreasing to 510.77g after heating, indicating a decrease in water quantity by 171.44g.

In the second location, the lowest moisture content was observed in sample AC02S-AB at 18.80%, while sample AC02S-B exhibited a moisture content of 20.93%. This suggests that deeper soil layers retain

more moisture, as soil texture can vary in water absorption and retention capabilities. This observation is supported by data from the particle size distribution table, which indicates a higher clay content in sample AC02S-B compared to AC02S-AB. The highest moisture content in the second location was recorded in sample AC02S-O, as the topmost layer receives the most rainfall. Differences in rainfall received by each soil layer can also contribute to variations in moisture content.

In the third location, Legeh, the lower layer was observed to be more humid than the upper layer, as indicated by the moisture content of sample LE03S-A (25.28%) compared to LE03S-B. Conversely, in Gemang, the highest moisture percentage was recorded at 22.94% in one sample and the lowest at 20.30% in another. This suggests that the upper soil layers in Gemang exhibit higher moisture content compared to Legeh, where the upper layers show lower moisture content.

The highest soil moisture content was recorded in the Dabong location, with sample DA05SO-A1 registering 20.95%. Conversely, the lowest moisture content was found in sample DA04SO-B2 at 11.71%. Interestingly, sample DA05SO-O did not record the highest moisture content, contrary to expectations based on typical patterns where the O layer usually exhibits higher moisture levels.

The highest moisture content in a sample was 36.06%, found in sample AC01SO, attributed to its high organic matter content. On the other hand, the lowest moisture content was 11.71%, observed in sample DA04S-B2 after drying, possibly due to its low clay content. Moisture content is a crucial factor in determining soil water content, affecting soil physical and chemical properties. The difference in moisture content before and after drying also reflects the water content in the sample, which plays a vital role in soil and organic matter analysis.

Moisture content in soil plays a significant role in determining soil health and its ability to support various biological, chemical, and physical processes essential for plant growth and ecosystem functioning. Adequate soil moisture is crucial for seed germination, root development, nutrient uptake, and overall plant health. In terms of physical properties, soil moisture affects soil structure and stability. Optimal moisture levels facilitate soil aggregation, creating pore spaces that promote root penetration, air exchange, and drainage. Conversely, excessive moisture can lead to soil compaction, waterlogging, and reduced oxygen availability, inhibiting root growth and microbial activity.

Furthermore, soil moisture influences nutrient availability and cycling. It helps dissolve and transport essential nutrients, making them accessible to plant roots. In moist conditions, microbial activity thrives, enhancing organic matter decomposition and nutrient mineralization. However, in excessively dry or waterlogged soils, microbial activity slows down, affecting nutrient release and soil fertility. Soil moisture also influences soil temperature regulation. Moist soils have higher heat capacity, buffering temperature fluctuations and providing a stable environment for soil organisms. Additionally, moisture affects soil erosion and runoff, impacting soil loss and nutrient leaching.

Overall, maintaining an optimal balance of soil moisture is critical for sustaining soil health and productivity. Proper water management practices, including irrigation, drainage, and soil conservation techniques, are essential for preserving soil moisture levels and ensuring long-term soil health and ecosystem resilience. In summary, the data indicates significant variations in soil moisture content across different locations, influenced by factors such as organic matter content (Van Geel et al., 2019), soil texture (Salter & Williams, 1965), soil layer (Li et al., 2020), and rainfall patterns. These findings underscore the importance of moisture content in understanding soil characteristics and its implications for agricultural practices and ecosystem management.

### 4.1.1 ORGANIC MATTER

The table shows the results of a loss-on-ignition test performed on 15 soil samples. The loss-on-ignition test is a common method for measuring the organic matter content of soil. It involves heating a soil sample to a high temperature (typically 550°C) in a crucible, and then measuring the mass loss. The mass loss is assumed to be due to the loss of organic matter, which is volatilized at high temperatures.

The data in the table shows that the soil samples have a wide range of organic matter content, from 5% to 71%. The highest organic matter content is found in the DAO4SO-O sample, while the lowest organic matter content is found in the ACO2SO-BH sample. The provided data, derived from a loss-on-ignition test on 15 soil samples, reveals a considerable diversity in organic matter content, ranging from 5% to 71%. This test, commonly employed in soil analysis, involves subjecting a soil sample to high temperatures to measure the mass loss, which is presumed to be indicative of organic matter volatilization. Among the samples, DAO4SO-O exhibits the highest organic matter content, while ACO2SO-BH has the lowest. The

variations in organic matter content can be attributed to several influential factors, notably the type of vegetation cover, climate conditions, and drainage characteristics.

All locations unanimously indicate that the O layer is higher, whether in Tebing Sg Chanal, Air Chanal, or Dabong, based on the sample data of AC01S-O (39%), AC02S0-O (17%), and DA04S-O (71%). The statement that the O horizon of soil is usually thicker than the underlying layers holds true in most cases. The O horizon typically consists of organic material formed from decomposing plant residues and other organic matter that accumulate at the soil surface. As a result, the O horizon tends to be thicker compared to the layers beneath it, which mainly consist of mineral material. This is because organic matter accumulates at the soil surface over time, continually adding to the thickness of the O horizon. Additionally, the decomposition of organic matter within the O horizon can contribute to its expansion and thickness. Conversely, the underlying layers primarily consist of mineral particles that are less prone to accumulation, resulting in thinner layers compared to the organic-rich O horizon. Therefore, the O horizon typically exhibits greater thickness relative to the underlying layers due to the continuous input of organic material and the slower rate of mineral accumulation beneath it. In contrast, soil layers A and B are typically composed of mineral soil particles that have undergone weathering and other physical and chemical processes. These layers may receive some organic inputs from the O horizon through processes like leaching or mixing by soil organisms, but they generally have lower organic matter content because the decomposition of organic materials is less active in these layers. Factors such as lower oxygen availability, reduced microbial activity, and physical protection of organic matter within soil aggregates contribute to the slower decomposition rates and lower organic matter content in soil layers A and B compared to the O horizon.

Vegetation cover plays a pivotal role. Soils enveloped by vegetation tend to exhibit higher organic matter content than those lacking such coverage. This discrepancy is often due to the decomposition of plant materials, contributing to the accumulation of organic matter in the soil. Moreover, climatic conditions exert a significant influence. Soils situated in warm and humid climates typically register higher organic matter content compared to those in cold and dry climates. The increased microbial activity and accelerated decomposition processes in warmer, moisture-rich environments contribute to elevated organic matter levels.

The drainage conditions of soil also contribute to the observed variations. Well-drained soils generally harbor higher organic matter content than poorly drained ones. Efficient drainage facilitates aerobic conditions, allowing for enhanced decomposition of organic materials.

Understanding the organic matter content of soil is crucial for assessing its fert ility. Organic matter plays a vital role in improving soil structure, promoting aeration, and augmenting water retention capacity. Additionally, it serves as a nutrient source for plants, influencing overall soil health and productivity. The substantial range in organic matter content among the soil samples underscores the complexity of factors shaping soil composition and highlights the importance of comprehensive soil analysis for informed agricultural and environmental management decisions.

### 4.1.2 Grain Size Soil

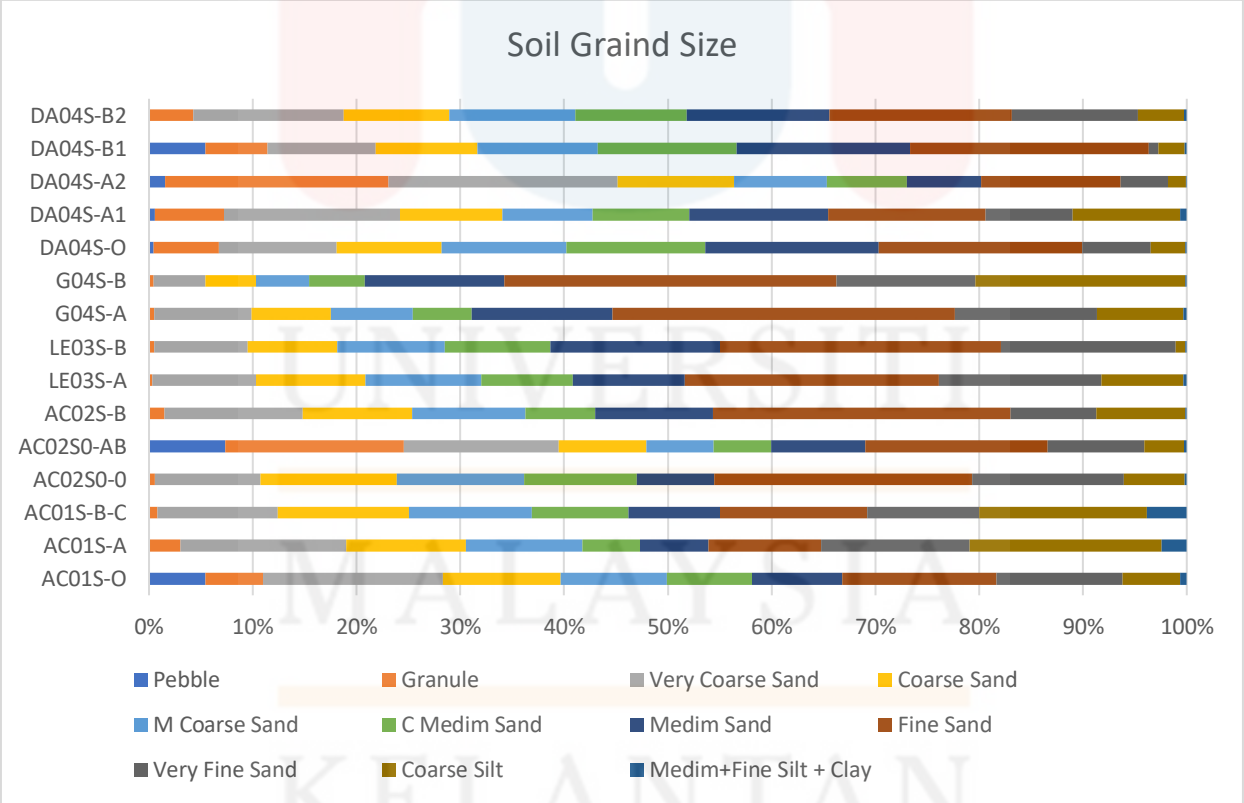


**Figure 4.2 : Soil Gaind Saiz in Soil Sample**

The soil particle size distribution is characterized by distinct categories based on the size of individual particles. Starting with pebbles and granules, which are larger than 4mm, the classification progresses through very coarse sand (2mm-4mm), coarse sand (1mm-2mm), medium coarse sand (710µm-1mm), medium sand (500µm-710µm), fine sand (355µm-500µm), very fine sand (125µm-250µm), coarse silt (63µm-125µm), and a combined category of medium and fine silt plus clay particles measuring less than 32µm. This systematic categorization of soil particles is essential for understanding soil texture, water retention, and other critical properties influencing soil behavior and fertility.

In sample AC01S-O, the dominant particle size falls within the 1mm-2mm range, comprising 17.36% of the total sample. This indicates a significant presence of medium-sized particles within this sample. Conversely, the <32µm size range represents the lowest percentage, accounting for only 0.63% of the total. These fine particles constitute a minor fraction of the sample's composition. Moving to sample AC01S-A, the highest percentage is found in the <32µm size range, constituting 18.49% of the total. This suggests a prevalence of very fine particles in this sample. Remarkably, there is no matter observed in the >4mm size range, indicating the absence of large particles. Similarly, in sample AC01S-B-C, the highest percentage is in the 63µm-125µm size range, representing 16.13% of the total. This suggests a substantial presence of particles within this size range. As with sample AC01S-A, there is no matter observed in the >4mm size range, indicating a lack of large particles.

In sample AC02S0-0, the highest percentage of particle size falls within the 125µm-250µm range, comprising 24.82% of the total sample. This indicates a substantial presence of particles within this size range. Notably, there is no matter observed in the >4mm size range, indicating the absence of larger particles in this sample. Moving to sample AC02S0-AB, the highest percentage is in the 125µm-250µm size range, representing 17.56% of the total. This suggests a significant presence of particles within this size range, similar to sample AC02S0-0. However, a small amount of matter is observed in the <32µm size range, constituting 0.27% of the total. Finally, in sample AC02S-B, the highest percentage is observed in the 250µm-355µm size range, accounting for 28.71% of the total. This indicates a substantial presence of medium-sized particles within this sample. Similar to AC02S0-0, there is no matter observed in the >4mm size range, indicating the absence of larger particles.

In sample LE03S-A, the highest percentage of particle size falls within the 250µm-355µm range, constituting 27.07% of the total sample. This indicates a significant presence of particles within this size range. Notably, there is no matter observed in the >4mm size range, indicating the absence of larger particles in this sample. Similarly, in sample LE03S-B, the highest percentage is observed in the 250µm-355µm size range, also accounting for 27.07% of the total. This suggests a substantial presence of particles within this size range, consistent with sample LE03S-A. However, a very small amount of matter is observed in the <32µm size range, constituting only 0.14% of the total.

In sample G04S-A, the predominant particle size falls within the 125µm-250µm range, constituting the highest percentage at 32.99% of the total sample. This indicates a substantial presence of particles within this size range. Conversely, the <32µm size range exhibits the lowest percentage, accounting for only 0.32% of the total. This suggests a minimal amount of finer particles in the sample. Similarly, in sample G04S-B, the highest percentage is observed in the 250µm-355µm size range, constituting 32.01% of the total sample. This indicates a notable presence of particles within this size range, albeit slightly larger than those in sample G04S-A. Conversely, the <32µm size range exhibits the lowest percentage, indicating a minimal presence of finer particles, with only 0.17% of the total falling within this range.

In sample DA04S-O, the predominant particle size falls within the 355µm-500µm range, constituting the highest percentage at 16.71% of the total sample. This indicates a notable presence of particles within this size range. Conversely, the <32µm size range exhibits the lowest percentage, indicating a minimal amount of finer particles, with only 0.15% of the total falling within this range. Similarly, in sample DA04S-A1, the highest percentage is observed in the 1mm-2mm size range, constituting 16.98% of the total sample. This indicates a significant presence of particles within this size range. Conversely, the 32µm-63µm size range exhibits the lowest percentage, indicating a minimal amount of particles within this range, with only 0.56% of the total falling within it. In sample DA04S-A2, the highest percentage is again observed in the 1mm-2mm size range, constituting 22.06% of the total sample, indicating a substantial presence of particles within this range. Conversely, the <32µm size range exhibits the lowest percentage, indicating a minimal presence of finer particles, with only 0.09% of the total falling within this range. Similarly, in samples DA04S-B1 and DA04S-B2, the highest percentage is observed in the 125µm-250µm size range, constituting 23.03% and 17.60% of the total sample, respectively, indicating a notable presence of particles within this size range. Conversely, the <32µm size range exhibits the lowest percentage in both samples, indicating minimal amounts of finer particles, with only 0.19% and 0.09% of the total falling

within this range, respectively. These findings highlight the diverse particle size distributions within the soil samples, underscoring the importance of understanding soil texture and its implications for various environmental processes.

Particle size plays a crucial role in determining soil health and its ability to support plant growth and ecosystem functions. Soil texture, which is determined by the relative proportions of sand, silt, and clay particles, influences various soil properties such as water retention, drainage, aeration, nutrient availability, and soil structure. Coarse-textured soils, dominated by larger sand particles, typically have good drainage and aeration due to the spaces between particles. However, they often struggle with water and nutrient retention as water easily drains away, and nutrients may leach below the root zone. On the other hand, fine-textured soils, rich in smaller clay particles, have high water and nutrient retention capacity but may suffer from poor drainage and aeration, leading to waterlogging and reduced oxygen availability for plant roots. The intermediate-sized silt particles contribute to soil fertility by enhancing nutrient retention and soil structure. Their ability to hold water and nutrients allows them to provide a stable environment for microbial activity and root growth. Moreover, soil structure, influenced by particle arrangement and aggregation, affects water infiltration, root penetration, and soil aeration.

Overall, a balanced combination of particle sizes, known as loam soil, is considered ideal for plant growth as it offers good drainage, water retention, aeration, and nutrient availability. Understanding the relationship between particle size distribution and soil health is crucial for effective soil management practices such as irrigation, fertilization, and soil conservation, ultimately supporting sustainable agriculture and ecosystem resilience.

### 4.1.3 REE

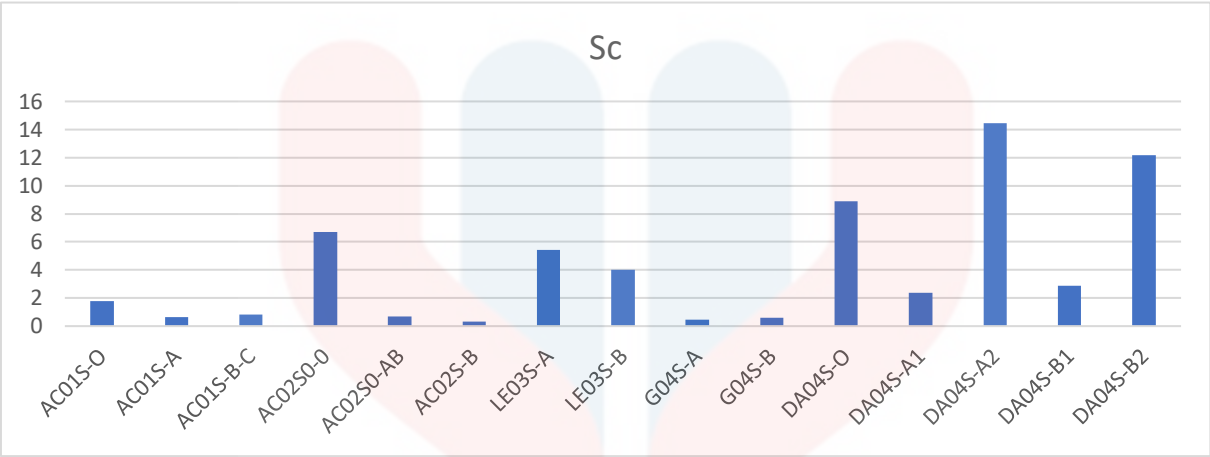


**Figure 4.3: Sc in Soil Sample**

In the first location, Tebing Sg Chanal, a total of 3,258 samples were recorded overall. Sample AC01S-O (organic layer) exhibited the highest quantity of Scandium (Sc), with a value of 1.775, while the lowest was found in sample AC01S-A (A layer) with only 0.657. Similarly, in the second location, sample AC02SO-O (O layer) showed a higher Sc content compared to other samples (soil layers A and B). In Legeh, the topsoil layer (soil layer A) in sample LE03S-A recorded a higher Sc value of 5.419 compared to the bottom layer (soil layer B) based on data from sample LE03S-B. However, in Gemang, the bottom layer (layer A) showed a higher Sc content, particularly in sample G04S-B with a record of 0.603. In Dabong, sample DA04S-A2 recorded the highest Sc value of 14.445.

The highest Sc content in the O horizon was recorded in sample DA04S-O at 8.8784, while the lowest was in sample AC01S-O with a record of 1.775. In layers A and B at all three locations, Sc values were <1, namely AC01S-A (1.775), AC01S-B-C (0.826), AC02S0-AB (0.693), AC02S-B (0.319), G04S-A (0.456), and G04S-B (0.603). The highest Sc value was found in sample DA04S-A2 with a record of 14.445, and the lowest was in AC02S-B at 0.319.

The average Sc in the O layers for all three samples was 5.7831, while in the A layers, it was 4.0043, and in the B layers, it was 3.4698. Human activities such as the use of fertilizers and pesticides can increase Sc content in the soil. Therefore, the O soil layer may have been exposed to these activities excessively compared to the A and B soil layers. The highest average was observed in Dabong, with a record of 8.0278,

likely due to the presence of abundant coal fly ash scattered on the soil surface in the Dabong area. Coal fly ash primarily consists of unburned organic matter residues (Chernoburova & Chagnes, 2021). The lowest average was in Gemang, which only obtained 0.5295.

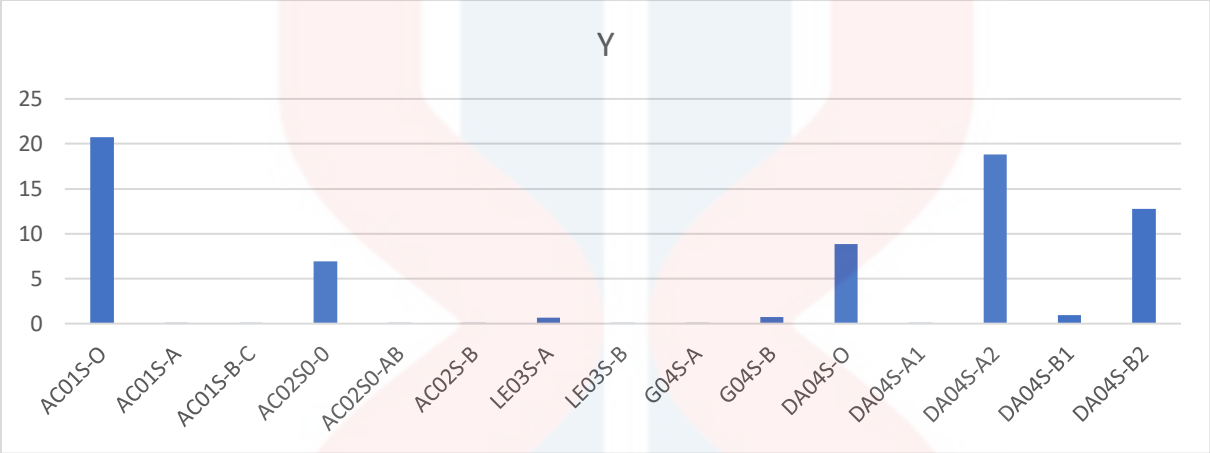


**Figure 4.4: Y Element in Soil Sample**

In Tebing Sg Chanal, the disparity between the highest recorded value in sample AC01S-O at 20.769 and the lowest value in sample AC01S-A at 0.09 highlights a notable concentration variation of Y, with higher levels observed in the upper layer. Similarly, in Air Chanal, the contrast between sample AC02S0-0's highest value at 6.913 and sample AC02S-B's lowest value at 0.077 indicates a significant difference in Y content, favoring the upper layer. Moving to Legeh, the comparison of sample LE03S-A's highest value at 0.684 and sample LE03S-B's lowest value at 0.108 underscores a similar trend of higher Y concentration in the upper layer compared to the lower layer. In Gemang, the difference between sample G04S-B's highest value at 0.724 and sample G04S-A's lowest value at 0.101 indicates a variation in Y distribution, with higher levels found in the upper layer. Lastly, in Dabong, the contrast between sample DA04S-A2's highest value at 18.829 and sample DA04S-B1's lowest value at 0.949 suggests a significant presence of Y in the middle layer, particularly higher in layer A compared to layers O and B. These observations imply potential geological and environmental factors influencing Y distribution within the soil profiles of these locations.

The average Y concentrations in the soil samples from Tebing Sungai Chanal, Air Chanal, Legeh, Gemang, and Dabong are 6.983, 2.364, 0.396, 0.4125, and 8.3096, respectively. Among these locations, Dabong exhibits the highest average Y content, suggesting that it may be a suitable site for Yttrium extraction activities. The significantly higher Y concentration in Dabong indicates a greater potential for

economic extraction compared to the other locations. Therefore, while Dabong presents a promising opportunity due to its higher Y content, a comprehensive assessment considering various factors is necessary to determine the most suitable location for Yttrium extraction activities.

The average Y concentrations in the O-horizon, A-horizon, and B-horizon layers are 12.1847, 3.3168, and 2.6054, respectively. This data indicates that the O-horizon layer generally has the highest Y content, followed by the A-horizon and then the B-horizon layers. The higher Y concentrations in the O-horizon layer can be attributed to the accumulation of organic matter and the deposition of Yttrium-rich materials over time. The A-horizon, which typically contains a mixture of organic and mineral material, also exhibits significant Y content but at a lower level compared to the O-horizon. Meanwhile, the B-horizon, consisting mainly of mineral material with limited organic content, has the lowest Y concentrations. Y content in the O-horizon is influenced by the accumulation of organic materials. As organic matter, such as decaying plant and animal residues, accumulates on the soil surface, it undergoes processes of weathering and decomposition. During these processes, organic compounds break down, releasing Yttrium and other elements into the soil solution. Yttrium, being present in organic matter or associated with organic compounds, becomes available for incorporation into the soil. Additionally, organic matter acts as a reservoir for Yttrium, gradually releasing it into the soil as decomposition progresses. This continual input and release of Yttrium from organic matter contribute to its higher concentrations in the O-horizon compared to other soil layers. Therefore, the dynamic interactions between organic matter and Yttrium cycling play a significant role in determining the Yttrium content in the O-horizon and ultimately influence soil fertility and ecosystem health.

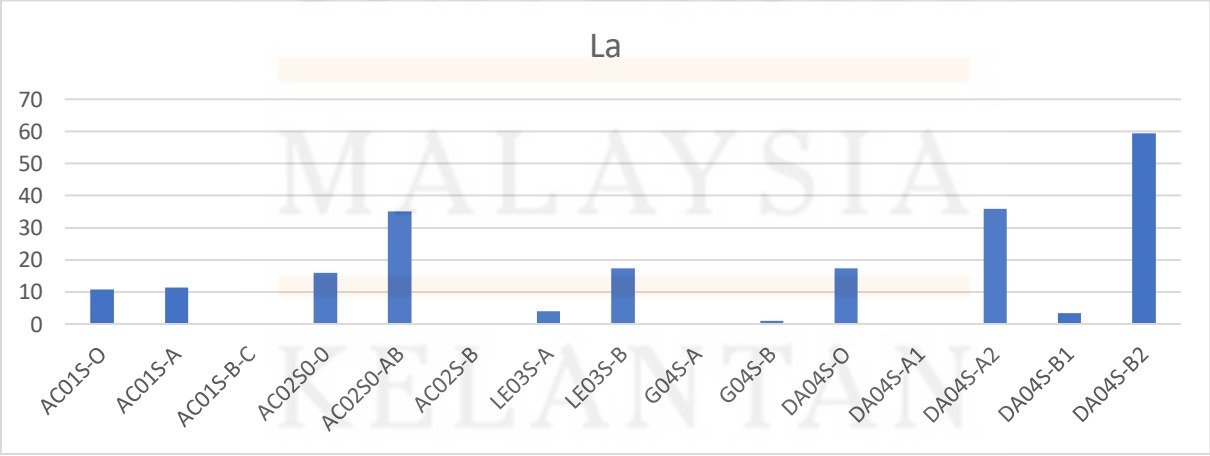


**Figure 4.5: La Element in Soil Sample**

In the dataset of lanthanum (La) concentrations across various soil samples, the highest value is recorded in sample DA04S-B2 at 59.489, indicating a significantly elevated level of lanthanum in that particular sample. Conversely, the lowest value is observed in sample AC01S-B-C at 0.039, suggesting a minimal presence of lanthanum in comparison. In Tebing Sg Chanal, the highest Lavalue is recorded in sample AC01S-A at 11.345, while the lowest is in sample AC01S-B-C at 0.039. For Air Chanal, sample AC02S0-AB exhibits the highest Lavalue at 35.083, whereas sample AC02S-B shows the lowest at 0.272. In Legeh, the highest Lavalue is found in sample LE03S-B at 17.393, with the lowest in sample LE03S-A at 4.067. Gemang records the highest Lavalue in sample G04S-B at 0.923 and the lowest in sample G04S-A at 0.0673. Lastly, in Dabong, sample DA04S-B2 presents the highest Lavalue at 59.489, while sample DA04S-A1 has the lowest at 0.024.

Additionally, the average La values for each location are provided. In Tebing Sg Chanal, the average Lavalue is 7.3513, whereas in Air Chanal, it is 17.1187. For Legeh, the average Lavalue is 10.73, and in Dabong, it is 23.206. lanthanum (La) extraction appears to be Dabong, as indicated by the significantly higher average La concentration compared to other locations. The average La concentration in Dabong is 23.206, considerably higher than in Tebing Sg Chanal (7.3513), Air Chanal (17.1187), and Legeh (10.73). Additionally, Dabong exhibits the highest recorded La concentration in sample DA04S-B2 at 59.489, further emphasizing its potential as a site for La extraction.

These averages indicate the typical concentrations of La within each layer across the sampled locations. The O-horizon, consisting of organic material and debris, has an average La concentration of 14.6413, slightly higher than the A-horizon's average concentration of 14.4067. Meanwhile, the B-horizon, which comprises the subsoil layer, exhibits the highest average La concentration at 16.2508. These findings suggest variations in La distribution within the soil profile, with the subsoil layer (B-horizon) generally containing higher La concentrations compared to the topsoil (A-horizon) and organic (O-horizon) layers.

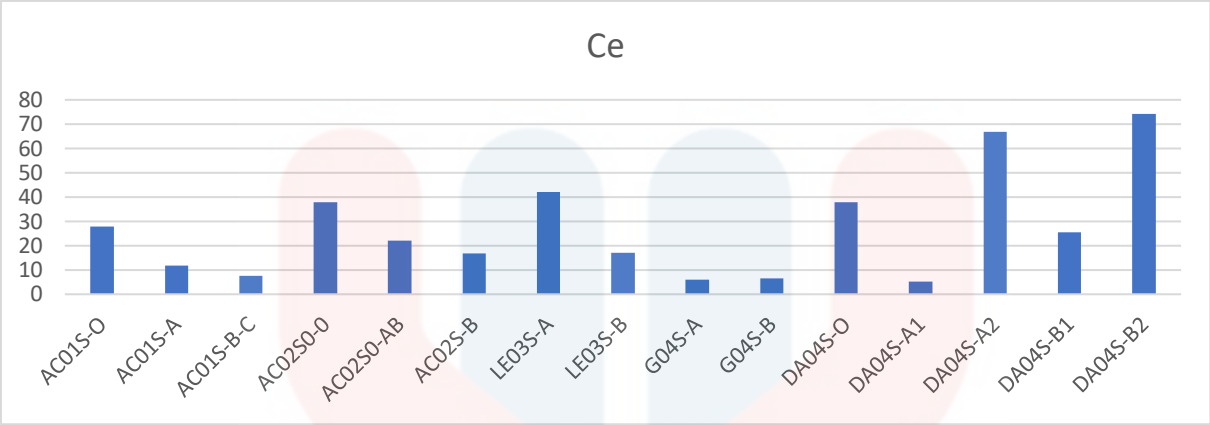


**Figure 4.6: Ce Element In soil Sample**

The overall cerium (Ce) concentrations exhibit a wide range, with the highest value recorded at 74.275 in sample DA04S-B2 and the lowest at 5.246 in DA04S-A1. In environments where conditions favor dissolution of Ce-containing minerals or organic matter, such as alkaline soils or reducing environments, Ce ions may be released into the soil solution. In alkaline environments, where conditions favor the presence of Ce4+, the less soluble Ce4+ ions are more prone to fixation onto secondary mineral structures like clay minerals or forming new phases such as cerianite (A Ghani et al., 2019). This fixation mechanism effectively traps cerium within the soil matrix, leading to its accumulation in specific layers, particularly in the B-horizon, where such mineralogical processes are more pronounced. Consequently, the higher Ce concentrations observed in the B-horizon samples across different locations could be attributed to the enhanced fixation and immobilization of Ce4+ ions within this layer due to its geochemical characteristics favoring cerium retention.

When considering individual samples across different locations, significant variability is observed. In Tebing Sungai Chanal, the highest Ce concentration is found in sample AC01S-A at 11.345, while the lowest is in sample AC01S-B-C at 0.039. Similarly, in Air Chanal, sample AC02S0-AB shows the highest Ce concentration at 35.083, contrasting sharply with sample AC02S-B, which has the lowest concentration at 0.272. In Legeh, sample LE03S-B exhibits the highest Ce concentration at 17.393, while sample LE03S-A has the lowest at 4.067. In Gemang, sample G04S-B records the highest concentration at 0.923, with sample G04S-A showing the lowest at 0.0673. Lastly, in Dabong, sample DA04S-B2 has the highest concentration at 59.489, while sample DA04S-A1 has the lowest at 0.024. When examining the average Ce concentrations for each location, considerable variation is evident. Tebing Sungai Chanal has an average Ce concentration of 7.6847, Air Chanal records 17.1187, Legeh shows 10.73, Gemang exhibits 0.49515, and Dabong records the highest average concentration at 23.206.

Further analysis reveals variations in Ce concentrations across different soil layers. In the O-horizon, sample DA04S-O shows the highest Ce concentration at 17.253. In the A-horizon, sample DA04S-A2 records the highest concentration at 35.854. Lastly, in the B-horizon, sample DA04S-B2 exhibits the highest Ce concentration at 59.489. On average, the O-horizon displays a concentration of 14.671, the A-horizon records 14.4067, and the B-horizon shows 16.2508. These findings underscore the spatial variability and distribution of Ce concentrations across soil layers and locations, highlighting the need for further investigation into the factors influencing these patterns.

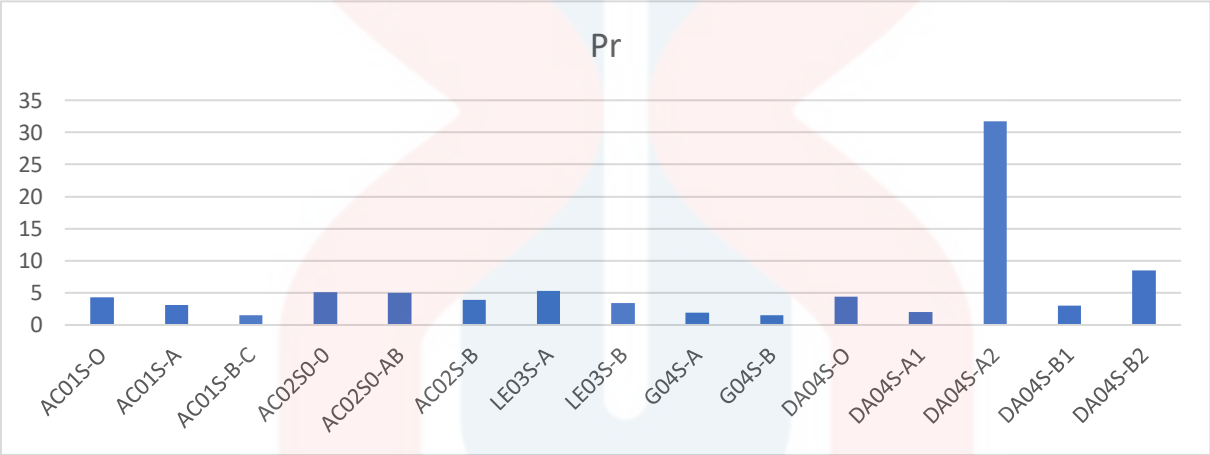


**Figure 4.7: Pr Element In soil Sample**

When examining Pr concentrations across different locations, notable variations are observed. In Tebing Sungai Chanal, the highest Pr concentration is found in sample AC01S-O at 4.31, whereas the lowest is in sample AC01S-B-C at 1.479. Similarly, in Air Chanal, sample AC02S0-0 exhibits the highest Pr concentration at 5.058, contrasting with the lowest concentration in sample AC02S-B at 3.909. In Legeh, the highest Pr concentration is in sample LE03S-A at 5.262, while the lowest is in sample LE03S-B at 3.382. For Gemang, sample G04S-A has the highest concentration at 1.904, with the lowest in sample G04S-B at 1.509. Dabong showcases the highest Pr concentration in sample DA04S-A2 at 31.701, whereas the lowest is in sample DA04S-A1 at 1.993. The average Pr concentrations for each location also vary. Tebing Sungai Chanal has an average of 3.6337, Air Chanal with 4.672, Legeh with 4.322, Gemang with 1.7065, and Dabong with 9.693.

Analyzing Pr concentrations based on soil layers reveals further insights. In the O-horizon, sample DA04S-O exhibits the highest concentration at 4.368. Conversely, in the A-horizon, sample DA04S-A2 records the

highest concentration at 31.701. The B-horizon sees the highest Pr concentration in sample DA04S-B2 at 8.515. The average Pr concentrations across soil layers show variations as well. The O-horizon has an average of 4.146, the A-horizon with 8.9475, and the B-horizon with 4.2025. These findings highlight the spatial variability of Pr concentrations across different soil layers and locations, reflecting the complex interplay of geological, geochemical, and environmental factors influencing Pr distribution in soil environments. Overall, the highest recorded concentration of Pr is 31.701 in sample DA04S-A2, while the lowest is G04S-B (1.509) . The physical characteristics of rocks, such as their porosity and permeability, can affect the movement and distribution of Pr within the soil profile, potentially leading to localized accumulation in areas with high rock content.

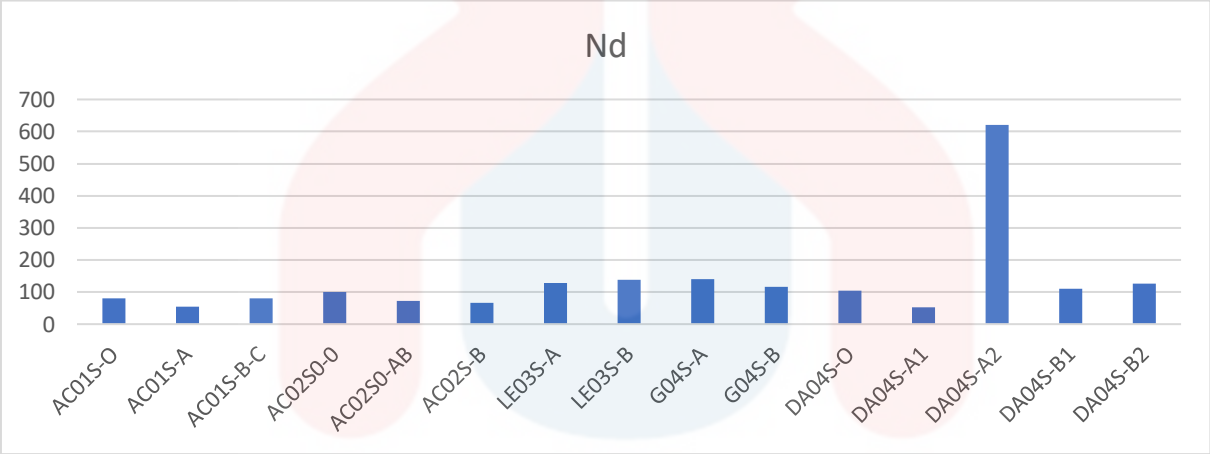


**Figure 4.8: Nd Element in Soil Sample**

The highest overall value of Nd concentration is recorded at 621.128, while the lowest is 51.516. Across different locations, the Nd concentration varies considerably. In Tebing Sungai Chanal, the highest concentration is found in sample AC01S-B-C at 79.528, while the lowest is in sample AC01S-A at 54.991. Similarly, in Air Chanal, sample AC02S0-0 exhibits the highest concentration at 100.366, and sample AC02S-B has the lowest at 66.971. In Legeh, sample LE03S-B has the highest Nd concentration at 138.395, whereas sample LE03S-A has the lowest at 128.653. Conversely, in Gemang, the highest concentration is observed in sample G04S-B at 116.904, with the lowest in sample G04S-A at 140.553. Notably, in Dabong, sample DA04S-A2 stands out with the highest Nd concentration at 621.128, contrasting starkly with sample DA04S-A1, which has the lowest concentration at 51.516. When examining the average values for each location, it is evident that Dabong has the highest average Nd concentration at 202.026, followed by Legeh at 133.524, Gemang at 128.7285, Air Chanal at 80.848, and Tebing Sungai Chanal at 71.9937.

Analyzing based on soil layers reveals interesting trends. The highest Nd concentration in layer O is recorded in sample DA04S-O at 104.521, while in layer A, it is notably higher, with sample DA04S-A2 exhibiting the highest concentration at 621.128. Layer B also shows relatively high concentrations, with sample DA04S-B2 recording the highest at 126.695. The varying concentrations of Nd can be attributed to several factors, including geological processes, weathering of parent materials, and anthropogenic activities. In Dabong, for instance, the exceptionally high concentration in sample DA04S-A2 may indicate geological conditions or mineral deposits that are rich in Nd. Conversely, lower concentrations in certain samples may result from factors such as leaching, erosion, or differences in soil composition. Additionally, anthropogenic activities like mining or industrial processes could contribute to the observed variations in Nd concentrations across different locations.

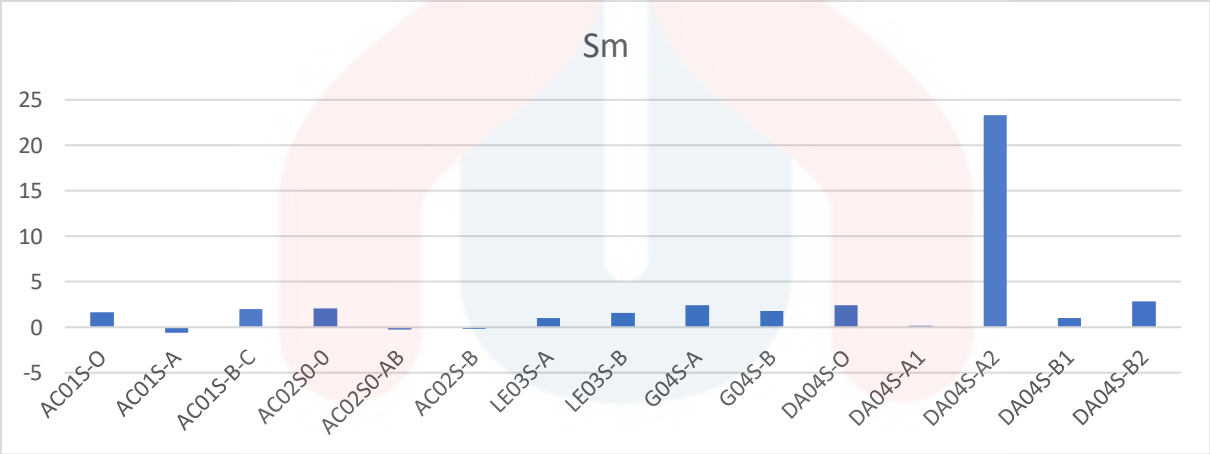


**Figure 4.9: Sm Element In Soil Sample**

The analysis of Samarium (Sm) concentrations reveals significant variations across the sampled locations. The highest recorded Sm concentration is 23.318, while the lowest is -0.59. Examining Sm concentrations across different locations provides valuable insights. In Tebing Sungai Chanal, sample AC01S-B-C exhibits the highest concentration at 1.964, while sample AC01S-A shows the lowest concentration at -0.59. Moving to Air Chanal, sample AC02S0-0 displays the highest Sm concentration at 2.076, contrasting with the lowest concentration found in sample AC02S0-AB at -0.28. In Legeh, sample LE03S-B exhibits the highest concentration at 2.416, whereas LE03S-A shows the lowest concentration at 1.022. Similarly, in Gemang, sample G04S-B displays the highest concentration at 2.405, while G04S-A exhibits the lowest concentration at 1.805. Finally, in Dabong, sample DA04S-O exhibits an exceptionally high Sm concentration at 23.318, whereas DA04S-A1 shows a lower concentration at 0.137. The average

Sm concentrations for each location vary, with Tebing Sungai Chanal recording 1.012, Air Chanal 0.832, Legeh 1.984, Gemang 2.105, and Dabong 4.748.

Considering Sm concentrations based on soil layers reveals distinct patterns. Sample DA04S-O exhibits the highest Sm concentration in the O-horizon at 23.318, while DA04S-B2 shows the highest concentration in the A-horizon at 2.85. In contrast, LE03S-B displays the highest Sm concentration in the B-horizon at 2.416. The average Sm concentrations for each soil layer also vary, with values of 8.14 for the O-horizon, 1.95 for both the A-horizon and B-horizon.

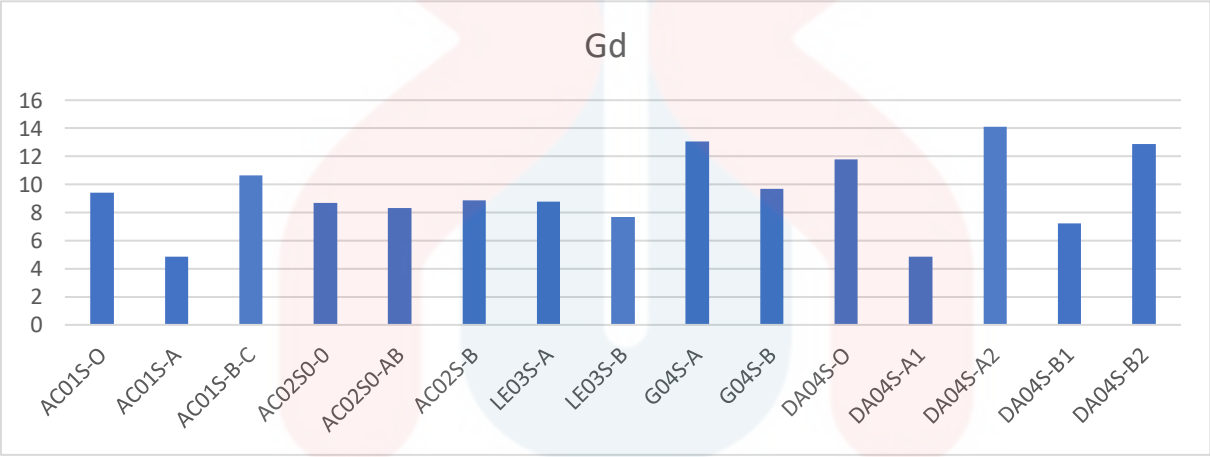


**Figure 4.10: Gd Element In Soil Sample**

The overall highest concentration of Gd is recorded at 14.0999, while the lowest is 4.877. Examining different locations reveals notable variations in Gd concentrations. In Tebing Sungai Chanal, sample AC01S-B-C exhibits the highest concentration at 10.648, contrasting with the lowest concentration found in sample AC01S-A at 4.877. Similarly, in Air Chanal, sample AC02S-B records the highest concentration at 8.886, while sample AC02S0-0 has the lowest at 8.708. In Legeh, the highest concentration is observed in sample LE03S-B at 13.066, with the lowest in sample LE03S-A at 8.798. In Gemang, sample G04S-B shows the highest concentration at 9.666, while sample G04S-A has the lowest at 7.698. Notably, in Dabong, sample DA04S-A2 stands out with the highest Gd concentration at 14.0999, in contrast to sample DA04S-A1, which has the lowest concentration at 4.85. Analyzing the average concentrations for each location, Legeh demonstrates the highest average Gd concentration at 10.432, followed closely by Dabong at 9.411, Tebing Sungai Chanal at 8.645, Gemang at 8.682, and Air Chanal at 8.634.

Further examination based on soil layers indicates interesting trends. The highest Gd concentration in layer O is recorded in sample DA04S-O at 11.764, while in layer A, it is highest in sample DA04S-A2 at 14.0999. Layer B also shows relatively high concentrations, with sample LE03S-B recording the highest at 13.066. The variations in Gd concentrations across different samples and locations may be influenced by

various factors such as geological processes, soil composition, and anthropogenic activities. The higher concentrations observed in certain samples could be indicative of geological formations or mineral deposits rich in Gd, while lower concentrations may result from factors like leaching, erosion, or differences in soil characteristics. Additionally, anthropogenic activities like mining or industrial processes may contribute to the observed variations in Gd concentrations.

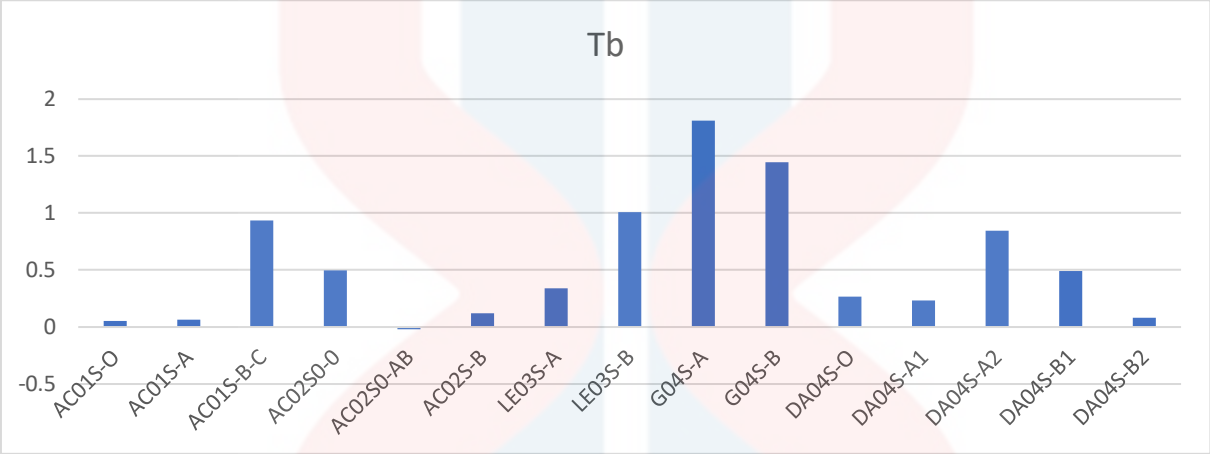


**Figure 4.11: Tb Element in Soil Sample**

Overall, the highest concentration of Tb recorded is 1.81, while the lowest is -0.019. Analyzing different locations reveals notable variations in Tb concentrations. In Tebing Sungai Chanal, sample AC01S-B-C exhibits the highest concentration at 0.934, contrasting with the lowest concentration found in sample AC01S-O at 0.053. Similarly, in Air Chanal, sample AC02S-B records the highest concentration at 0.119, while sample AC02S0-AB has the lowest at -0.019. In Legeh, the highest concentration is observed in sample LE03S-B at 1.009, with the lowest in sample LE03S-A at 0.341. In Gemang, sample G04S-A shows the highest concentration at 1.81, while sample G04S-B has the lowest at 1.445. Notably, in Dabong, sample DA04S-A1 stands out with the highest Tb concentration at 0.233, in contrast to sample DA04S-B1, which has the lowest concentration at 0.084. Analyzing the average concentrations for each location, Gemang demonstrates the highest average Tb concentration at 1.6275, followed by Legeh at 0.675, Dabong at 0.4902, Tebing Sungai Chanal at 0.344, and Air Chanal at 0.198.

Further examination based on soil layers indicates interesting trends. The highest Tb concentration in layer O is recorded in sample AC01S-B-C at 0.934, while in layer A, it is highest in sample G04S-A at 1.81. Layer B also shows relatively high concentrations, with sample G04S-B recording the highest at 1.445. In the O layer, which represents the surface organic horizon, the average Tb concentration is 0.174. Moving down to layer A, which typically comprises the mineral topsoil, the average Tb concentration

increases to 0.536. In layer B, representing the subsoil horizon beneath the topsoil, the average Tb concentration remains relatively high at 0.5405.

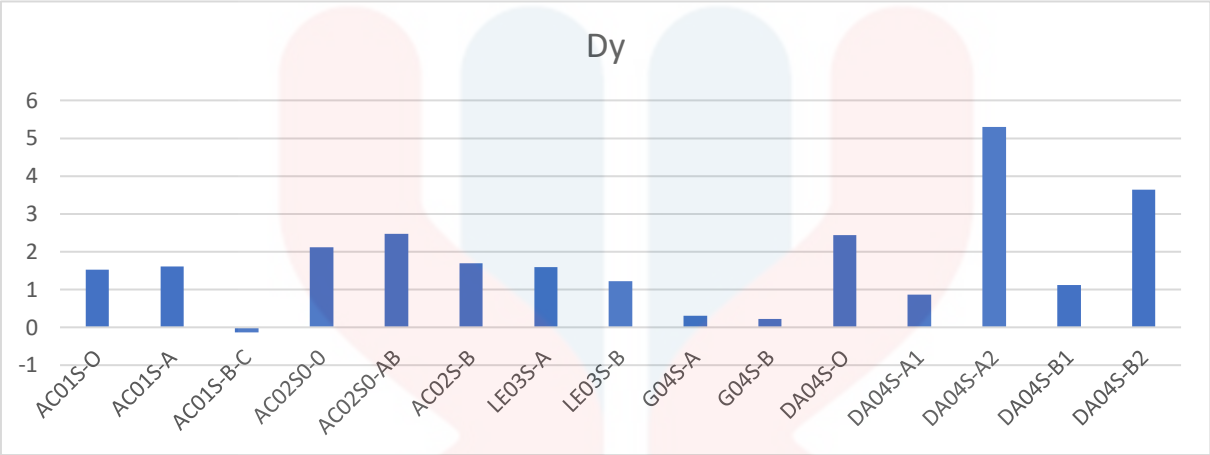


**Figure 4.12: Dy Element in Soil Sample**

The analysis of Dysprosium (Dy) concentrations reveals notable variations across the sampled locations. The highest recorded Dy concentration is 5.291, while the lowest is -0.14. Examining Dy concentrations across different locations provides valuable insights. In Tebing Sungai Chanal, samples AC02S0-0 and AC02S0-AB exhibit the highest concentrations at 2.116 and 2.466, respectively, while the lowest concentration is observed in sample AC01S-B-C at -0.14. Moving to Air Chanal, sample DA04S-O shows the highest Dy concentration at 2.435, contrasting with the lowest concentration found in sample G04S-B at 0.22. Similarly, in Legeh, sample AC01S-A displays the highest concentration at 1.607, whereas G04S-B again exhibits the lowest concentration at 0.22. In Gemang, the highest Dy concentration is recorded in sample G04S-A at 0.307. Finally, in Dabong, sample DA04S-B1 exhibits the highest Dy concentration at 3.647. The average Dy concentrations for each location vary, with Tebing Sungai Chanal recording 0.795, Air Chanal 1.174, Legeh 1.1, Gemang 0.3135, and Dabong 2.038.

Considering Dy concentrations based on soil layers reveals distinct patterns. Sample DA04S-O exhibits the highest Dy concentration in the O-horizon at 2.435, while AC01S-A shows the highest concentration in the A-horizon at 1.607. In contrast, sample DA04S-B1 displays the highest Dy concentration in the B-horizon at 3.647. The average Dy concentrations for each soil layer also vary, with values of 1.383 for the O-horizon, 1.174 for the A-horizon, and 2.174 for the B-horizon. These findings underscore the spatial and vertical variability in Dy concentrations across the sampled locations, highlighting the importance of comprehensive soil analysis for understanding elemental distribution and potential environmental implications.

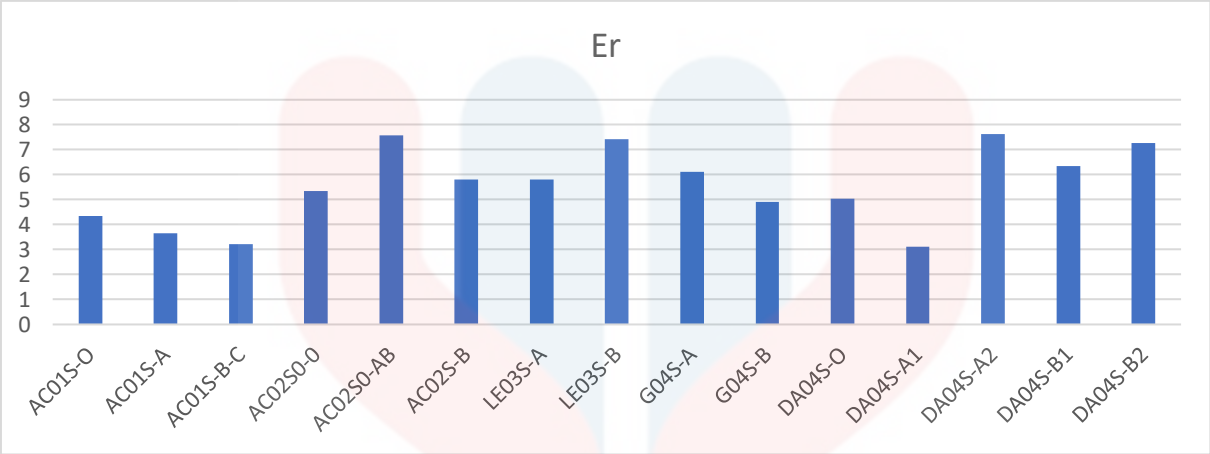


**Figure 4.13: Er Element in Soil Sample**

The overall highest concentration of Er is recorded at 7.632, while the lowest is at 3.103. These values represent the extremes observed across all samples and layers, indicating the range of Er concentrations present in the study area. Analyzing the Er concentrations across different locations provides insights into spatial variations. For instance, in Tebing Sungai Chanal, the highest Er concentration is found in sample AC01S-O at 4.344, while the lowest is in sample AC01S-B-C at 3.224. Similarly, in Air Chanal, sample AC02S0-AB exhibits the highest concentration at 7.584, contrasting with sample AC02S0-0, which has the lowest concentration at 5.356. In Legeh, the Er concentration ranges from 7.422 in sample LE03S-B to 5.798 in sample LE03S-A. In Gemang, sample G04S-A records the highest Er concentration at 6.125, while sample G04S-B shows the lowest at 4.914. Lastly, in Dabong, sample DA04S-O exhibits the highest Er concentration at 5.024, whereas sample DA04S-A1 has the lowest at 3.103. Assessing the average Er concentrations across locations further elucidates trends. Tebing Sungai Chanal has an average Er concentration of 3.7387, while Air Chanal records a higher average at 6.249. Legeh exhibits an average Er concentration of 6.610, while Gemang and Dabong show averages of 5.5195 and 5.719, respectively.

Examining the Er concentrations across soil layers highlights variations vertically within the soil profile. In the O layer, sample AC02S0-0 shows the highest concentration at 5.356, while in the A layer, sample AC02S0-AB records the highest at 7.584. In the B layer, sample G04S-A exhibits the highest concentration at 6.125. Starting with the O layer, the average Er concentration is calculated at 4.574. Moving to the A layer, the average Er concentration increases to 5.684. This suggests a higher accumulation of Er within the A horizon, which is characterized by a mixture of organic and mineral material. The

elevated Er levels in this layer may be attributed to the accumulation of Er-bearing minerals or the downward movement of Er from the O horizon through leaching and mineral weathering processes.

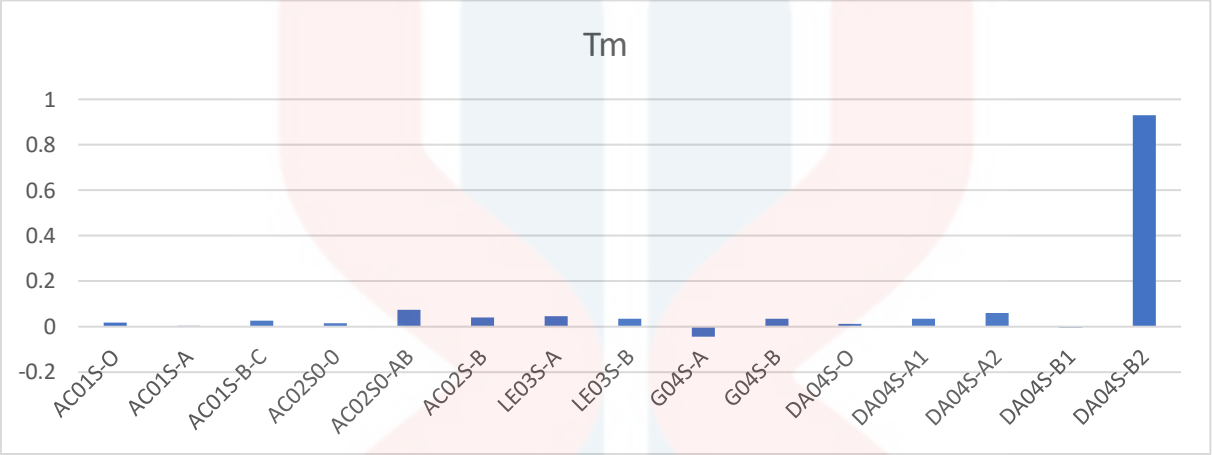


**Figure 4.14: Tm Element in Soil Sample**

The overall analysis of the element Tm (thulium) concentrations reveals that the highest recorded value is 0.93, while the lowest is -0.045. Examining Tm concentrations across various soil samples within different locations provides insightful observations. In Tebing Sungai Chanal, sample DA04S-O exhibits the highest Tm concentration at 0.012, contrasting with the lowest concentration recorded in sample AC01S-A at 0.005. Moving to Air Chanal, sample DA04S-B1 displays the highest concentration at 0.034, while the lowest concentration is observed in sample LE03S-B, also at 0.034. Similarly, in Legeh, sample DA04S-A2 shows the highest concentration at 0.059, with the lowest concentration again found in sample LE03S-B at 0.034. In Gemang, a significant contrast is evident, with sample DA04S-B2 recording the highest concentration at 0.93, while sample G04S-B displays the lowest at -0.045. Similarly, in Dabong, sample DA04S-B2 and G04S-B exhibit the highest and lowest concentrations, respectively, mirroring the findings in Gemang. The average Tm concentrations for each location vary, with Tebing Sungai Chanal recording 0.015, Air Chanal 0.019, Legeh 0.028, Gemang 0.174, and Dabong 0.174.

Considering Tm concentrations based on soil layers reveals consistent patterns, with sample DA04S-B2 exhibiting the highest concentration across all soil layers (O, A, and B), each registering 0.93. The average Tm concentrations for each soil layer remain consistent across locations, with values of 0.015 for the O-horizon, 0.019 for the A-horizon, and 0.028 for the B-horizon. These findings highlight spatial and vertical variations in Tm concentrations within the soil profiles of the sampled locations, emphasizing

the importance of comprehensive soil analysis for understanding elemental distribution and potential ecological implications.

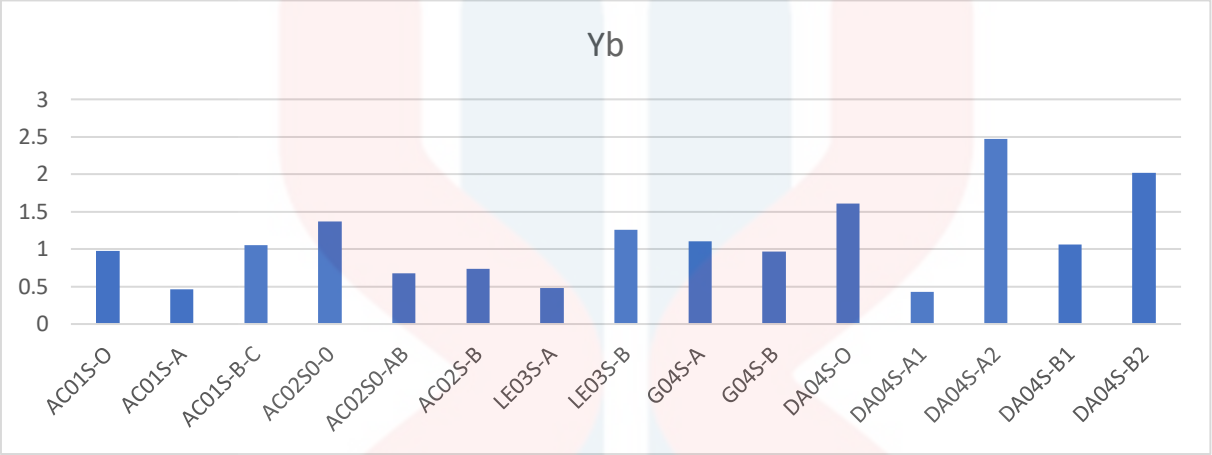


**Figure 4.15: Yb Element in Soil Sample**

The provided data outlines the highest and lowest concentrations of the element Yb (ytterbium) both overall and within specific soil samples across various locations. The highest overall concentration of Yb is recorded at 2.475, while the lowest is 0.429. When considering Yb concentrations within samples based on location, notable variations are observed. In Tebing Sungai Chanal, sample AC01S-B-C exhibits the highest Yb concentration at 1.055, whereas sample DA04S-A1 has the lowest at 0.429. In Air Chanal, sample AC02S0-0 records the highest concentration at 1.373, while AC02S0-AB has the lowest at 0.675. Similarly, in Legeh, sample LE03S-B shows the highest concentration at 1.108, with LE03S-A displaying the lowest at 0.479. In Gemang, sample G04S-B has a concentration of 0.97, while G04S-A has a significantly higher concentration at 1.606. Lastly, in Dabong, sample DA04S-O records the highest concentration at 1.606, contrasting with DA04S-A1, which has the lowest at 0.429. Furthermore, the average Yb concentrations for each location provide additional insights. Tebing Sungai Chanal has an average concentration of 0.8193, Air Chanal records 0.928, Legeh has 0.793, Gemang exhibits 1.29, and Dabong has 1.198.

Considering Yb concentrations based on soil layers reveals further trends. In the O-horizon, sample DA04S-O displays the highest concentration at 1.606, while in the A-horizon, sample DA04S-B2 records the highest concentration at 2.018. Lastly, in the B-horizon, sample G04S-A exhibits the highest concentration at 1.606. The average Yb concentrations for each soil layer indicate that the O-horizon generally has the highest average concentration at 1.354, followed by the A-horizon at 1.394, and the B-

horizon at 1.155. These findings suggest spatial variability in Yb concentrations across different soil layers and locations, underscoring the importance of comprehensive soil analysis in understanding the distribution and potential impacts of Yb in terrestrial ecosystems.

# CHAPTER 5

# CONCLUSIONS AND RECOMMENDATIONS

## 5.1 Conclusions

Based on the analysis of multiple rare earth elements (REEs) including yttrium (Y), lanthanum (La), cerium (Ce), praseodymium (Pr), neodymium (Nd), samarium (Sm), gadolinium (Gd), terbium (Tb), dysprosium (Dy), thulium (Tm), and ytterbium (Yb) across various soil samples from different locations, it is evident that there exists a significant spatial and vertical variability in the distribution of these elements within the soil profiles. The study highlights the intricate interplay of geological, geochemical, and environmental factors influencing the concentrations of REEs in terrestrial ecosystems. Spatially, different locations exhibit distinct patterns of REE concentrations, with some areas showing higher concentrations than others, suggesting localized sources or geological formations rich in these elements. Additionally, variations in REE concentrations are observed vertically within the soil profile, with differences between soil layers indicating the influence of processes such as organic matter accumulation, mineral weathering, and leaching.

## 5.2 Recommendations

Investing in research and development (R&D) of alternative extraction and processing technologies, alongside the discovery of new rare earth mineral deposits, holds immense potential to revolutionize the rare earth industry and foster sustainability in resource utilization. Traditional extraction methods for rare earth elements (REEs), such as acid leaching and solvent extraction, often involve harsh chemicals and generate significant environmental pollution. By investing in R&D, innovative and environmentally friendly extraction techniques can be developed. These may include bioleaching, where microorganisms are employed to selectively extract REEs from ores, or hydrometallurgical processes that utilize less toxic reagents and minimize waste generation

# REFERENCES

*Soil is the thin layer of material covering the earth's surface*. (2020, February 27). Australian Environmental Education. https://www.australianenvironmentaleducation.com.au/education-resources/what-is-soil/

Mihajlovic, J., Bauriegel, A., Stärk, H.-J., Roßkopf, N., Zeitz, J., Milbert, G., & Rinklebe, J. (2019). Rare earth elements in soil profiles of various ecosystems across Germany. *Applied Geochemistry: Journal of the International Association of Geochemistry and Cosmochemistry*, *102*, 197–217. https://doi.org/10.1016/j.apgeochem.2019.02.002

Michael E. Ritter. (2021, October 1). Geosciences LibreTexts; Libretexts. https://geo.libretexts.org/Bookshelves/Geography_(Physical)/The_Physical_Environment_(Ritter)/11%3A_Soil_Systems/11.04%3A_Soil_Profiles

Albrecht, M. (2015, July 22). *Rare Earth Elements vs. Rare Metals: an overview*. Linkedin.com. https://www.linkedin.com/pulse/rare-earth-elements-vs-metals-overview-mike-albrecht-p-e-/

Yusoff, Z. M., Ngwenya, B. T., & Parsons, I. (2013). Mobility and fractionation of REEs during deep weathering of geochemically contrasting granites in a tropical setting, Malaysia. *Chemical Geology*, *349–350*, 71–86. https://doi.org/10.1016/j.chemgeo.2013.04.016

Fisher, M. R. (2017). 9.1 soil profiles & processes. In *Environmental Biology*. Open Oregon Educational Resources.

Zhenghua, W., Jun, L., Hongyan, G., Xiaorong, W., & Chunsheng, Y. (2001). Adsorption isotherms of lanthanum to soil constituents and effects of pH, EDTA and fulvic acid on adsorption of lanthanum onto goethite and humic acid. *Chemical Speciation and Bioavailability*, *13*(3), 75–81. https://doi.org/10.3184/095422901782775444

Anak Rebu, S. I., Abdirahman Siyad, S., Ab Malik Marwan, N. F., Shaari Majed, F. F., Shafiee, N. S., & Sulaiman, N. (2023). Rare earth distribution in Batu Melintang Granitic Rocks, Jeli, Kelantan. *BIO Web of Conferences*, *73*, 04014. https://doi.org/10.1051/bioconf/20237304014

Earle, S., & Earle, S. (2015). 3.3 crystallization of magma. In *Physical Geology*. BCcampus.

Alexandra Bot, 2024,*The importance of soil organic matter* from https://www.fao.org/3/a0100e/a0100e.pdf

Van Es, F. M. A. H. (2021). Building Soil for Better Crops Ecological Management For Healthy Soil.

Sandra Brown, Asim Biswas, Jean Caron, Miles Dyck, and Bing Si (2021). Geosciences LibreTexts; Libretexts. https://geo.libretexts.org/Bookshelves/Soil_Science/Digging_into_Canadian_Soils%3A_An_Introduction_to_Soil_Science/01%3A_Digging_In/1.04%3A_Soil_Physics

Rocchi, I., Coop, M. R., & Maccarini, M. (2017). The effects of weathering on the physical and mechanical properties of igneous and metamorphic saprolites. *Engineering Geology*, *231*, 56–67. https://doi.org/10.1016/j.enggeo.2017.10.003

Yu, C., Högfors-Rönnholm, E., Stén, P., Engblom, S., & Åström, M. E. (2023). Iron-sulfur geochemistry and acidity retention in hydrologically active macropores of boreal acid sulfate soils: Effects of mitigation suspensions of fine-grained calcite and peat. *The Science of the Total Environment*, *856*(159142), 159142. https://doi.org/10.1016/j.scitotenv.2022.159142

kosthilaire. (2015, April 4). *Grain size distribution*. Geotechinal Portfolio. https://kosthilaire8162.wordpress.com/2015/04/04/grain-size-distribution/

Chen, J., Liao, J. B., & Wei, C. H. (2014). Wei: Chinese J Anal Lab. *Chinese J Anal Lab. Forum*, *33*, 803–807.

Jian, H. L., Yin, X. Q., & Zhang, J. F. (2007). Zhang: Chinese J Spectrosc Lab. *Chinese J Spectrosc Lab. Forum*, *24*, 138–141.

Liang, S. X., Wang, X., & Wu, H. (2012). Spectrosc Spect Anal. *Spectrosc Spect Anal. Forum*, *32*, 809–812.

Qiu, Z., Zhang, J., Liu, C., Li, F., & Wu, Z. (2016). Comparison of different microwave digestion methods for heavy metals from stream sediment. *Proceedings of the 2016 International Conference on Advances in Energy, Environment and Chemical Science*. https://www.researchgate.net/publication/304480063_Comparison_Of_Different_Microwave_Digestion_Methods_For_Heavy_Metals_From_Stream_Sediment

Rogers, J. R., & Bennett, P. C. (2004). Mineral stimulation of subsurface microorganisms: release of limiting nutrients from silicates. *Chemical Geology*, *203*(1–2), 91–108. https://doi.org/10.1016/j.chemgeo.2003.09.001

*Rare earth elements*. (n.d.). Rareelementresources.com. Retrieved February 4, 2024, from https://www.rareelementresources.com/rare-earth-elements

Linert, W., Bridge, M., & Ohtaki, H. (2003). Solvation. In *Comprehensive Coordination Chemistry II* (pp. 597–610). Elsevier.

https://doi.org/10.1016/B0-08-043748-6/01159-2

Wall, F. (2021). Rare Earth Elements. In *Encyclopedia of Geology* (pp. 680–693). Elsevier.

https://doi.org/10.1016/B978-0-08-102908-4.00101-6

Hoshino, M., Sanematsu, K., & Watanabe, Y. (2016). REE Mineralogy and Resources. In B. Jean-Claude & P. Vitalij K. (Eds.), *Including Actinides* (Vol. 49, pp. 129–291). Elsevier.

Matusiewicz, H. (Ed.). (2019). WET DIGESTION METHODS .researchgate.net https://www.researchgate.net/profile/Arvind_Singh56/post/Dose_anybody_know_if_there_is_any_book_or_article_gives_a_comprehensive_and_systematic_introduction_to_the_selection_of_acids_used_in_wet_digestion/attachment/5a10e1abb53d2f46c7eb0887/AS%3A562222876368896%401511055787836/download/chapter13.pdf

Wilschefski, S., & Baxter, M. (2019). Inductively coupled plasma mass spectrometry: Introduction to analytical aspects. *The Clinical Biochemist Reviews*, *40*(3), 115–133. https://doi.org/10.33176/aacb-19-00024

Van Geel, M., Yu, K., Peeters, G., van Acker, K., Ramos, M., Serafim, C., Kastendeuch, P., Najjar, G., Ameglio, T., Ngao, J., Saudreau, M., Castro, P., Somers, B., & Honnay, O. (2019). Soil organic matter rather than ectomycorrhizal diversity is related to urban tree health. *PloS One*, *14*(11), e0225714. https://doi.org/10.1371/journal.pone.0225714

Salter, P. J., & Williams, J. B. (1965). The influence of texture on the moisture characteristics of soils: I. A critical comparison of techniques for determining the available-water capacity and moisture characteristic curve of a soil. *Journal of Soil Science*, *16*(1), 1–15. https://doi.org/10.1111/j.1365-2389.1965.tb01416.x

Li, Z., Vanderborght, J., & Smits, K. M. (2020). The effect of the top soil layer on moisture and evaporation dynamics. *Vadose Zone Journal: VZJ*, *19*(1). https://doi.org/10.1002/vzj2.20049

Chernoburova, O., & Chagnes, A. (2021). The future of scandium recovery from wastes. *International Conference on Raw Materials and Circular Economy*, *5*, 55.

A Ghani, A., Shahjamal, M., Ng, T. F., Ismail, N. E. H., Mohamad Zulkifley, M. T., Islami, N., Quek, L. X., Abu Bakar, A. F., Amir Hassan, M. H., Abdul Aziz, J. H., & Masor, A. F. (2019). Ce anomaly in I-type granitic soil from kuantan, peninsular Malaysia: Retention of zircon in the weathering product. *Sains Malaysiana*, *48*(2), 309–315. https://doi.org/10.17576/jsm-2019-4802-06

## APPENDIX A

| SAMPLE | WEIGHTING BAT (g) | SAMPLE WEIGHT(g) | | MOISTURE (%) |
|---|---|---|---|---|
| | | BEFORE | AFTER | |
| AC01SO | 12.24 | 211.84 | 135.45 | 36.06 |
| AC01S-A | 12.53 | 702.21 | 510.77 | 27.26 |
| AC01S-B | 12.54 | 588.71 | 449.45 | 23.66 |
| AC02S0-O | 12.34 | 515.9 | 403.67 | 21.75 |
| AC02S-AB | 12.21 | 522.13 | 423.96 | 18.80 |
| AC02S-B | 12.17 | 723.6 | 572.15 | 20.93 |
| G04S0-A | 12.25 | 753.35 | 580.54 | 22.94 |
| G04S0-B | 12.34 | 822.11 | 655.26 | 20.30 |
| LE03S-A | 12.36 | 651.44 | 486.73 | 25.28 |
| LE03S-B | 12.34 | 822.11 | 582.92 | 29.09 |
| DA04S0-O | 12.45 | 1326.13 | 1084.3 | 18.24 |
| DA05S0-A1 | 12.56 | 1609.37 | 1272.15 | 20.95 |
| DA05S0-A2 | 12.53 | 2185.22 | 1738.52 | 20.44 |
| DA05S0-B1 | 12.55 | 1782.19 | 1572.31 | 11.78 |
| DA05S0-B2 | 12.6 | 920.92 | 813.1 | 11.71 |

Moisture persentage in Soil Sample

| Sample | Crucible weight (g) | Sample weight (g) | Mass of crucible+ sample | Mass of organic matter in soil (g) | Loss-on-ignition (%) |
|---|---|---|---|---|---|
| ACOISO | 21.0085 | 0.1266 | 21.1351 | 21.0856 | 39 |
| AC02SO-A | 19.9874 | 0.1155 | 20.1029 | 20.0652 | 32 |
| ACOIC-B | 16.7904 | 0.1067 | 16.8971 | 16.882 | 14 |
| ACO2SO-O | 25.7794 | 0.105 | 25.8844 | 25.8658 | 17 |
| ACO2SO-AB | 15.9511 | 0.1791 | 16.1302 | 16.1062 | 13 |
| ACO2SO-B | 21.921 | 0.1316 | 22.0526 | 22.0449 | 5 |
| GO4SO-A | 24.5619 | 0.1933 | 24.7552 | 24.7231 | 16 |
| GO4SO-B | 20.7146 | 0.1114 | 20.826 | 20.807 | 17 |
| LE03S0-A | 17.6005 | 0.1037 | 17.7042 | 17.6868 | 16 |
| LE03S0-B | 19.0323 | 0.1386 | 19.1709 | 19.143 | 20 |
| DAO4SO-O | 19.3986 | 0.1302 | 19.5288 | 19.4359 | 71 |
| DAO4SO-AI | 20.4745 | 0.1792 | 20.6537 | 20.6321 | 12 |
| DAO4SO-AII | 23.7217 | 0.1466 | 23.8683 | 23.848 | 13 |
| DAO4SO-BI | 17.467 | 0.1854 | 17.6524 | 17.6364 | 8 |
| DAO4SO-BII | 22.668 | 0.1877 | 22.8557 | 22.8387 | 9 |

Organic matter contant in soil sample

| SOIL | Pebble | Granule | Very Coarse Sand | Coarse Sand | M Coarse Sand | C Medim Sand | Medim Sand | Fine Sand | Very Fine Sand | Coarse Silt | Medim+ Fine Silt + Clay | Total |
|---|---|---|---|---|---|---|---|---|---|---|---|---|
| | >4mm | 2mm-4mm | 1mm-2mm | 710µm-1mm | 500µm-710µm | 355µm-500µm | 250µm-355µm | 125µm-250µm | 63µm-125µm | 32µm-63µm | <32µm | |
| AC01S-O | 5.46 | 5.51 | 17.36 | 11.31 | 10.29 | 8.19 | 8.68 | 14.84 | 12.18 | 5.55 | 0.63 | 100.00 |
| AC01S-A | 0.00 | 3.02 | 15.97 | 11.56 | 11.20 | 5.54 | 6.61 | 10.85 | 14.35 | 18.49 | 2.41 | 100.00 |
| AC01S-B-C | 0.00 | 0.83 | 11.59 | 12.62 | 11.84 | 9.31 | 8.83 | 14.20 | 10.81 | 16.13 | 3.85 | 100.00 |
| AC02S0-0 | 0.00 | 0.56 | 10.20 | 13.11 | 12.27 | 10.86 | 7.49 | 24.82 | 14.66 | 5.86 | 0.18 | 100.00 |
| AC02S0-AB | 7.36 | 17.16 | 14.96 | 8.44 | 6.46 | 5.57 | 9.05 | 17.56 | 9.30 | 3.85 | 0.27 | 100.00 |
| AC02S-B | 0.00 | 1.48 | 13.33 | 10.52 | 10.96 | 6.70 | 11.34 | 28.71 | 8.24 | 8.57 | 0.16 | 100.00 |
| LE03S-A | 0.00 | 0.30 | 10.02 | 10.56 | 11.12 | 8.86 | 10.77 | 24.50 | 15.63 | 7.95 | 0.30 | 100.00 |
| LE03S-B | 0.00 | 0.51 | 9.01 | 8.64 | 10.32 | 10.19 | 16.34 | 27.07 | 16.88 | 0.90 | 0.14 | 100.00 |
| G04S-A | 0.00 | 0.48 | 9.40 | 7.66 | 7.86 | 5.69 | 13.59 | 32.99 | 13.66 | 8.35 | 0.32 | 100.00 |
| G04S-B | 0.00 | 0.45 | 4.98 | 4.89 | 5.10 | 5.38 | 13.46 | 32.01 | 13.36 | 20.20 | 0.17 | 100.00 |
| DA04S-O | 0.46 | 6.30 | 11.33 | 10.10 | 12.02 | 13.40 | 16.71 | 19.60 | 6.62 | 3.31 | 0.15 | 100.00 |
| DA04S-A1 | 0.56 | 6.64 | 16.98 | 9.90 | 8.64 | 9.33 | 13.40 | 15.16 | 8.41 | 10.34 | 0.64 | 100.00 |
| DA04S-A2 | 1.56 | 21.51 | 22.06 | 11.26 | 8.92 | 7.70 | 7.16 | 13.47 | 4.58 | 1.69 | 0.09 | 100.00 |
| DA04S-B1 | 5.45 | 5.97 | 10.40 | 9.84 | 11.55 | 13.42 | 16.70 | 23.03 | 0.88 | 2.56 | 0.19 | 100.00 |
| DA04S-B2 | 0.09 | 4.16 | 14.48 | 10.21 | 12.15 | 10.74 | 13.73 | 17.60 | 12.11 | 4.57 | 0.15 | 100.00 |

Grind Size of soil sample in persentage

| | AC01S-O | AC01S-A | AC01S-B-C | AC02S0-O | AC02S0-AB | AC02S-B | LE03S-A | LE03S-B | G04S-A | G04S-B | DA04S-O | DA04S-A1 | DA04S-A2 | DA04S-B1 | DA04S-B2 |
|---|---|---|---|---|---|---|---|---|---|---|---|---|---|---|---|
| Sc | 1.775 | 0.657 | 0.826 | 6.696 | 0.693 | 0.319 | 5.419 | 4.004 | 0.456 | 0.603 | 8.8784 | 2.356 | 14.445 | 2.897 | 12.17 |
| Y | 20.769 | 0.09 | 0.091 | 6.913 | 0.101 | 0.077 | 0.684 | 0.108 | 0.101 | 0.724 | 8.872 | 0.096 | 18.829 | 0.949 | 12.802 |
| La | 10.67 | 11.345 | 0.039 | 16.001 | 35.083 | 0.272 | 4.067 | 17.393 | 0.0673 | 0.923 | 17.253 | 0.024 | 35.854 | 3.41 | 59.489 |
| Ce | 27.791 | 11.679 | 7.642 | 37.804 | 22.09 | 16.931 | 42.015 | 17.086 | 6.092 | 6.611 | 37.753 | 5.246 | 66.895 | 25.493 | 74.275 |
| Pr | 4.31 | 3.1111 | 1.479 | 5.058 | 5.049 | 3.909 | 5.262 | 3.382 | 1.904 | 1.509 | 4.368 | 1.993 | 31.701 | 2.969 | 8.515 |
| Nd | 79.461 | 54.991 | 79.528 | 100.366 | 73.207 | 66.971 | 128.653 | 138.395 | 140.553 | 116.904 | 104.521 | 51.516 | 621.128 | 110.773 | 126.695 |
| Sm | 1.662 | -0.59 | 1.964 | 2.076 | -0.28 | -0.221 | 1.022 | 1.553 | 2.416 | 1.805 | 2.405 | 0.137 | 23.318 | 1.042 | 2.85 |
| Gd | 9.411 | 4.877 | 10.648 | 8.708 | 8.31 | 8.886 | 8.798 | 7.698 | 13.066 | 9.666 | 11.764 | 4.85 | 14.0999 | 7.246 | 12.871 |
| Tb | 0.053 | 0.064 | 0.934 | 0.495 | -0.019 | 0.119 | 0.341 | 1.009 | 1.81 | 1.445 | 0.269 | 0.233 | 0.843 | 0.49 | 0.084 |
| Dy | 1.522 | 1.607 | -0.14 | 2.116 | 2.466 | 1.686 | 1.593 | 1.226 | 0.307 | 0.22 | 2.435 | 0.865 | 5.291 | 1.111 | 3.647 |
| Er | 4.344 | 3.648 | 3.224 | 5.356 | 7.584 | 5.807 | 5.798 | 7.422 | 6.125 | 4.914 | 5.024 | 3.103 | 7.632 | 6.334 | 7.267 |
| Tm | 0.018 | 0.005 | 0.026 | 0.016 | 0.074 | 0.04 | 0.046 | 0.034 | -0.045 | 0.034 | 0.012 | 0.034 | 0.059 | -0.004 | 0.93 |
| Yb | 0.977 | 0.466 | 1.055 | 1.373 | 0.675 | 0.738 | 0.479 | 1.26 | 1.108 | 0.97 | 1.606 | 0.429 | 2.475 | 1.064 | 2.018 |

REE contant in soil profile

## APPENDIX B


Tebing Sg Chanal Soil Profile 1 B-C

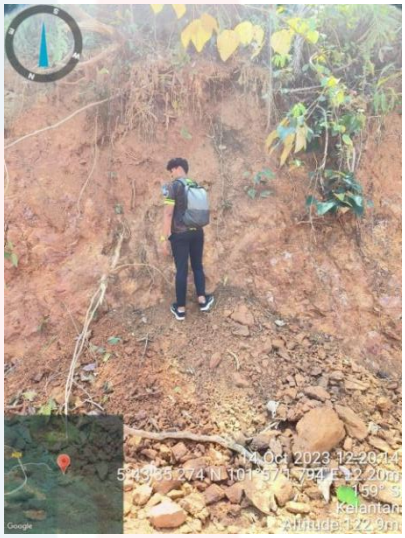

Tebing Sg Chanal Soil Profile 1 B-C


Air Chanal Soil Profile 2

Legeh Soil Profile


Legeh Soil Profile Far View


Gemang Soil Layer A


Gemang Soil Layer B


Gemang Soil Layer A


Gemang Soil Layer B